

University of Windsor

## Scholarship at UWindor

---

Electronic Theses and Dissertations

Theses, Dissertations, and Major Papers

---

1-1-1974

### Inelastic collisions between excited atoms and molecules; Sensitized fluorescence and quenching in mixtures of potassium and cesium with nitrogen, hydrogen, deuterium hydride and deuterium.

Daniel A. McGillis  
*University of Windsor*

Follow this and additional works at: <https://scholar.uwindsor.ca/etd>

---

#### Recommended Citation

McGillis, Daniel A., "Inelastic collisions between excited atoms and molecules; Sensitized fluorescence and quenching in mixtures of potassium and cesium with nitrogen, hydrogen, deuterium hydride and deuterium." (1974). *Electronic Theses and Dissertations*. 6048.

<https://scholar.uwindsor.ca/etd/6048>

This online database contains the full-text of PhD dissertations and Masters' theses of University of Windsor students from 1954 forward. These documents are made available for personal study and research purposes only, in accordance with the Canadian Copyright Act and the Creative Commons license—CC BY-NC-ND (Attribution, Non-Commercial, No Derivative Works). Under this license, works must always be attributed to the copyright holder (original author), cannot be used for any commercial purposes, and may not be altered. Any other use would require the permission of the copyright holder. Students may inquire about withdrawing their dissertation and/or thesis from this database. For additional inquiries, please contact the repository administrator via email ([scholarship@uwindsor.ca](mailto:scholarship@uwindsor.ca)) or by telephone at 519-253-3000ext. 3208.

INELASTIC COLLISIONS BETWEEN EXCITED ATOMS AND MOLECULES;  
SENSITIZED FLUORESCENCE AND QUENCHING IN MIXTURES OF K AND Cs  
WITH N<sub>2</sub>, H<sub>2</sub>, HD AND D<sub>2</sub> .

by

Daniel A. McGillis

A Thesis  
Submitted to the Faculty of Graduate Studies through the Department  
of Physics in Partial Fulfillment of the Requirements for  
the Degree of Doctor of Philosophy at the  
University of Windsor

Windsor, Ontario

1967

UMI Number: DC52611

### INFORMATION TO USERS

The quality of this reproduction is dependent upon the quality of the copy submitted. Broken or indistinct print, colored or poor quality illustrations and photographs, print bleed-through, substandard margins, and improper alignment can adversely affect reproduction.

In the unlikely event that the author did not send a complete manuscript and there are missing pages, these will be noted. Also, if unauthorized copyright material had to be removed, a note will indicate the deletion.

**UMI**®

---

UMI Microform DC52611

Copyright 2008 by ProQuest LLC.

All rights reserved. This microform edition is protected against unauthorized copying under Title 17, United States Code.

ProQuest LLC  
789 E. Eisenhower Parkway  
PO Box 1346  
Ann Arbor, MI 48106-1346

ABX 6326

APPROVED BY:

L. Krause

Dr. L. Krause (Chairman)

F. Holuj

Dr. F. Holuj

J. Huschilt

Dr. J. Huschilt

Approved by letter tk.

Dr. J. C. Polanyi  
University of Toronto  
(External Examiner)

181352

ABSTRACT

${}^2P_{1/2} \text{ --- } {}^2P_{3/2}$  mixing and  ${}^2P_J \text{ --- } {}^2S_{1/2}$  quenching in potassium and cesium vapors, induced by collisions with  $N_2$ ,  $H_2$ , HD and  $D_2$ , were studied using techniques of sensitized fluorescence. The mixtures of alkali vapors with the various gases, in which the alkali vapor pressure was kept low to avoid radiation trapping, were irradiated with one component of the appropriate resonance doublet. The fluorescence which contained both components of the doublet, was monitored at right angles to the direction of excitation. The measurements of the relative intensities of the fluorescent components yielded the total inelastic cross sections for  ${}^2P$  mixing,  $Q_{12}({}^2P_{1/2} \text{ --- } {}^2P_{3/2})$ ,  $Q_{21}({}^2P_{1/2} \text{ --- } {}^2P_{3/2})$ , and quenching,  $Q_{10}({}^2P_{1/2} \text{ --- } {}^2S_{1/2})$ ,  $Q_{20}({}^2P_{3/2} \text{ --- } {}^2S_{1/2})$ . In the case of potassium the quenching cross sections for  $N_2$ ,  $H_2$ , HD and  $D_2$  were:  $Q_{10} = 35, 7, 11, 2 (\text{\AA})^2$  and  $Q_{20} = 39, 4, 14, 1 (\text{\AA})^2$ , respectively. For the cesium resonance states the corresponding quenching cross sections were:  $Q_{10} = 62, 7, 4, 8 (\text{\AA})^2$  and  $Q_{20} = 100, 5, 3, 7 (\text{\AA})^2$ , respectively. The potassium -  $N_2$ ,  $H_2$ , HD and  $D_2$  mixing cross sections were found to be:  $Q_{12} = 99.7, 75.6, 74.0, 72.2 (\text{\AA})^2$  and  $Q_{21} = 66.0, 53.2, 50.4, 48.7 (\text{\AA})^2$ , respectively, only slightly larger than the corresponding potassium-inert gas cross sections. The cesium -  $N_2$ ,  $H_2$ , HD and  $D_2$  mixing cross sections were:  $Q_{12} = 4.7, 6.7, 4.8, 4.2 (\text{\AA})^2$  and  $Q_{21} = 25.2, 43.8, 32.1, 27.8 (\text{\AA})^2$ , respectively, five orders of magnitude larger than the cesium-inert gas mixing cross sections.

The quenching results are consistent with the intermediate complex theories of quenching in which energy matching between the atomic and molecular states is of no importance. The  $^2P$  mixing cross sections do, however, exhibit a marked dependence on the rotational structure of the colliding molecules. The results are discussed in terms of induced rotational transitions on the basis of which the cross sections ( $Q_{21}$ ) for mixing in cesium induced by ortho and para hydrogen are calculated.

### ACKNOWLEDGMENTS

I wish to thank Professor L. Krause for suggesting this problem and for his supervision and support throughout the course of this work. I should like also to thank the members of the Atomic Physics Group for many profitable discussions.

Acknowledgments are due to Mr. W. Eberhart for his skill in constructing the fluorescence tubes and supporting glasswork.

I am also indebted to the Province of Ontario for its financial support in the form of Graduate Fellowships.

Finally, I am grateful to my wife and parents for their understanding and encouragement.

TABLE OF CONTENTS

	Page
ABSTRACT	iii
ACKNOWLEDGMENTS	v
LIST OF TABLES	viii
LIST OF FIGURES	ix
I. INTRODUCTION	1
II. RATE EQUATIONS FOR THE SENSITIZED FLUORESCENCE AND QUENCHING PROCESSES	6
III. DESCRIPTION OF THE APPARATUS	12
IV. EXPERIMENTAL PROCEDURE	17
V. SENSITIZED FLUORESCENCE AND QUENCHING IN MIXTURES OF POTASSIUM WITH N <sub>2</sub> , H <sub>2</sub> , HD AND D <sub>2</sub>	20
A. The K - N <sub>2</sub> Collision Cross Sections	20
B. The K - H <sub>2</sub> , K - HD and K - D <sub>2</sub> Collision Cross Sections	24
VI. SENSITIZED FLUORESCENCE AND QUENCHING IN MIXTURES OF CESIUM WITH N <sub>2</sub> , H <sub>2</sub> , HD AND D <sub>2</sub>	29
VII. DISCUSSION OF THE RESULTS	35
A. Accuracy of the Results	35
B. The Quenching Cross Sections	36
C. The <sup>2</sup> P Mixing Cross Sections	40
APPENDICES	
A. EXPERIMENTAL DATA	48
B. ITERATIVE METHOD OF CALCULATING THE COLLISION NUMBERS Z <sub>ab</sub>	59
C. CALCULATION OF THE QUENCHING CROSS SECTIONS Q <sub>10</sub> AND Q <sub>20</sub> FROM η-VALUES	60

	Page
BIBLIOGRAPHY	61
VITA AUCTORIS	63

LIST OF TABLES

	Page
I. Mean Lifetimes and Wavelengths Associated with the Potassium and Cesium $^2P$ States	19
II. Cross Sections for Excitation Transfer in K - Molecule Collisions	28
III. Cross Sections for Quenching in K - Molecule Collisions	28
IV. Cross Sections for Excitation Transfer in Cs - Molecule Collisions	34
V. Cross Sections for Quenching in Cs - Molecule Collisions	34
VI. Reported Quenching Cross Sections for K - Molecule Collisions at Different Relative Velocities $V_r$	37
VII. Calculated Cross Sections for $^2P_{1/2} \leftarrow ^2P_{3/2}$ Mixing in Cs Induced by o- $H_2$ and p- $H_2$ Collisions	45

LIST OF FIGURES

		Page
1.	Energy Levels Involved in Sensitized Fluorescence and in the Quenching of Alkali Metal Resonance Radiation Induced in Collisions with Molecules	6
2.	Schematic Diagram of Apparatus	12
3.	The Fluorescence Tube	14
4.	Plots of Intensity Ratios $\eta_1$ and $\eta_2$ Against $N_2$ Pressure Showing Sensitized Fluorescence in Potassium	20
5.	Plots of Intensity Ratios $I_0/I$ Against $N_2$ Pressure Showing Collisional De-excitation Involving Both Quenching and $2P_{1/2} - 2P_{3/2}$ Mixing Processes	21
6.	Plots of Collision Numbers $Z_{10}$ and $Z_{12}$ Against $N_2$ Pressure	23
7.	Plots of Intensity Ratios $\eta_1$ Against $H_2$ , HD and $D_2$ Pressures	25
8.	Plots of Intensity Ratios $\eta_2$ Against $H_2$ , HD and $D_2$ Pressures	25
9.	Plots of Intensity Ratios $I_0/I$ Against $D_2$ Pressure	26
10.	Plots of Collision Numbers $Z_{10}$ and $Z_{12}$ Against $D_2$ Pressure	27
11.	Plots of Intensity Ratios $\eta_1$ and $\eta_2$ Against $N_2$ Pressure Showing Sensitized Fluorescence in Cesium	30
12.	Plots of Intensity Ratios $\eta_1$ Against $H_2$ , HD and $D_2$ Pressures	31
13.	Plots of Intensity Ratios $\eta_2$ Against $H_2$ , HD and $D_2$ Pressures	32
14.	Plots of Collision Numbers $Z_{12}$ and $Z_{21}$ Against $H_2$ Pressure	33

## I INTRODUCTION

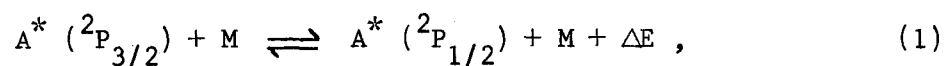
The transfer of excitation between the resonance states of alkali metal atoms during atomic collisions, termed collision induced mixing, is perhaps the most thoroughly investigated energy transfer process occurring between neutral atoms<sup>1</sup>. The determination of the alkali-inert gas mixing cross sections has received the greatest attention since they are of considerable importance in optical pumping experiments in which inert gases are used as buffers. It was felt that it would be interesting to extend these measurements to include the mixing induced by collisions with diatomic molecules.

Wood and Mohler<sup>2</sup> in 1918 observed that the ratio of the sodium D-line intensities emitted by fluorescing sodium vapor changed when a small amount of H<sub>2</sub> was mixed with the vapor. Lochte-Holtgreven<sup>3</sup> (1928) confirmed these observations and measured the D-line ratio as a function of H<sub>2</sub>, N<sub>2</sub> and other gas pressures. These were the first indications that non-equilibrium populations of the alkali resonance levels could be altered by molecular collisions but since these early semi-quantitative experiments there has been no systematic study of this effect.

The present research concerns itself with the determination of the cross sections for mixing between the  $^2P_{1/2}$  and  $^2P_{3/2}$  resonance levels of potassium and cesium induced by diatomic molecule collisions. Since each level is connected to the ground state by an optically

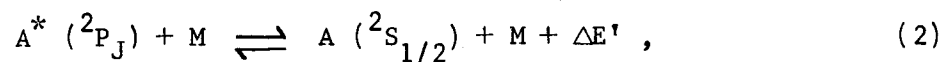
allowed transition, a study of sensitized fluorescence can be used to investigate the mixing process.

When one of the resonance levels of an alkali atom is excited by the absorption of radiation of the appropriate wavelength, this excitation may be collisionally transferred to the other level and the atom will then emit radiation of a wavelength different than that used for the excitation. In other words, fluorescence is sensitized by the collision through a radiationless transfer of excitation between the resonance levels. If no such effective collision occurred, the excited atom would re-radiate the absorbed light as resonance fluorescence. The mixing induced in the  $^2P$  state of an excited alkali atom  $A^*$  by a collision with a diatomic molecule  $M$  may be described by the following equation:



where  $\Delta E$ , the energy difference between the fine structure components, is supplied or carried away by the various degrees of freedom of the colliding partners. This energy defect ranges from  $58 \text{ cm}^{-1}$  (0.007 eV) for potassium to  $554 \text{ cm}^{-1}$  (0.07 eV) for cesium.

Using molecules to induce  $^2P$  mixing complicates the interpretation of sensitized fluorescence experiments since molecules are known to be very efficient in causing radiationless decay to the ground state<sup>4-6</sup>. This quenching reaction may be written as:



where the energy released,  $\Delta E'$ , is equal to the excitation energy of  $A^*$ .

Thus there is the possibility that even though excitation is transferred from one resonance level to another, the sensitized fluorescence will be reduced by subsequent quenching collisions. In order to account for such occurrences the quenching cross section of the molecule M must be known for each resonance level.

Quenching of cesium fluorescence has not yet been studied and although the cross sections for quenching of potassium resonance radiation by  $N_2$ ,  $H_2$  and  $D_2$  have been reported<sup>7-9</sup>, in no case were the resonance levels resolved. It was therefore necessary to investigate concurrently quenching and mixing collisions.

There have been many theoretical attempts to interpret the mixing process induced by atomic collisions<sup>10</sup>. It might be expected that since molecules generally possess permanent multipole moments and have more degrees of freedom than atoms, they would induce mixing with greater efficiencies than those predicted by the current atom-atom collision theories but there has not been, apparently, any explicit theoretical treatment of  $^2P$  mixing induced by molecular collisions. The bulk of the relevant atom-molecule work has centered on the quenching process and, though most of the theories are of an empirical nature, the ideas they contain may shed some light on the mixing problem.

The high efficiency with which molecules de-excite the electronic states of atoms has been attributed to the involvement of the internal molecular degrees of freedom in a process of energy transfer. It would be expected from classical considerations that the cross section for collisional transfer of energy between atomic electrons

and the nuclear motion of the quenching molecule would be very small. In order to explain the large de-excitation probabilities in atom-molecule collisions, it has been suggested that a close energy match between the downward electronic and the upward molecular transitions would lead to an efficient resonant transfer of energy. Kallmann and London<sup>11</sup> (1929) and Morse and Stuckelberg<sup>12</sup> (1931) have considered such resonant processes from the quantum mechanical viewpoint. Calculations based on idealized potential energy curves have shown that the energy transfer cross section depends on the nature of the interaction between the colliding partners, on the relative velocity before the collision, and on the energy difference between the electronic and molecular transitions. The conditions under which the resonance effect might be important have been examined by Dickens, Linnett and Sovers<sup>13</sup> (1962) who calculated theoretical cross sections for the quenching of excited sodium and mercury by various molecules on the basis of a model in which the potential energy curves did not cross. The results indicated that although resonance would enhance the transfer probability, it could not by itself lead to large de-excitation cross sections. Polanyi<sup>14</sup> (1967) has shown, for the first time, that vibrational excitation does indeed occur in quenching collisions ( $\text{Hg}^* + \text{CO}$ ) but that resonance between the electronic and vibrational transitions is of no importance in the energy exchange.

Rice<sup>15</sup> (1931) proposed that electronic quenching should be regarded as a transition between intersecting potential surfaces and Magee and Rice<sup>16</sup> (1941) and Laidler<sup>17</sup> (1942) have attempted theoretical

calculations based on this concept. Both treatments describe  $\text{Na}^* + \text{H}_2$  quenching in terms of a relatively stable complex. Quenching proceeds by way of an ionic potential surface which has quasi-intersections with the surfaces of the reactants and products. There has been a number of other proposals that intermediate complex formation with subsequent intersystem crossings or quasi-crossings is responsible for quenching<sup>18,19</sup>. However, detailed knowledge of the relevant potential energy surfaces is lacking and for this reason there has been no comprehensive theoretical treatment of the quenching reaction.

The main purpose of this research is to provide a firm experimental basis for a better understanding of inelastic atom-molecule collision processes.

II. RATE EQUATIONS FOR THE SENSITIZED FLUORESCENCE  
AND QUENCHING PROCESSES

The processes that take place when a mixture of alkali vapor and molecular gas is irradiated continuously with the  $D_2$ -component\* of the alkali resonance doublet, are shown schematically in Fig. 1. The solid arrows indicate transitions giving rise to sensitized fluorescence and the broken arrows represent collisional deactivation of the  $^2P$  alkali atoms to the ground state, which manifests itself by the quenching of resonance radiation.

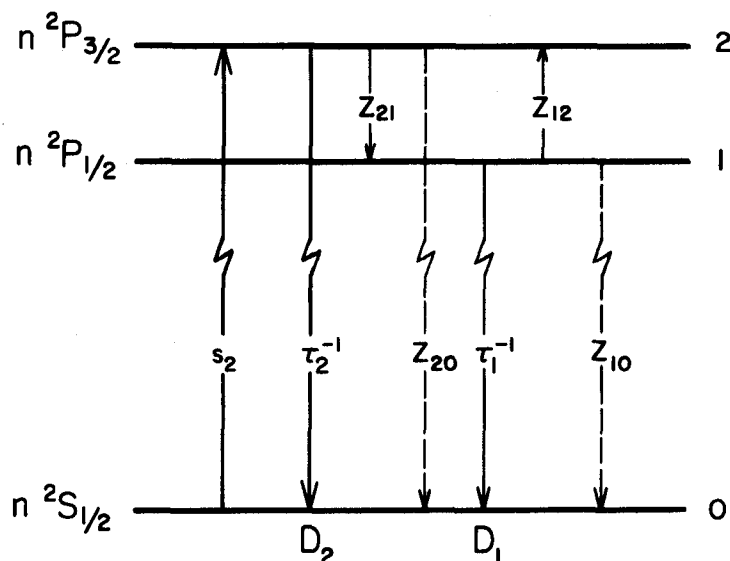
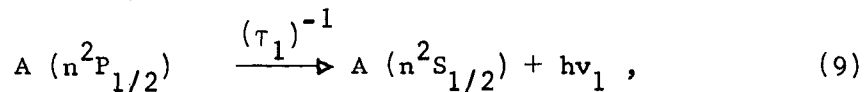
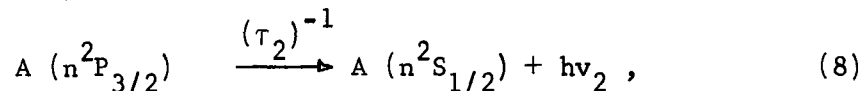
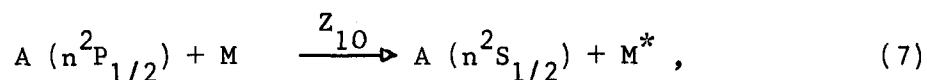
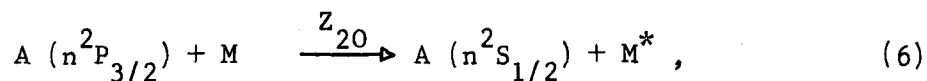
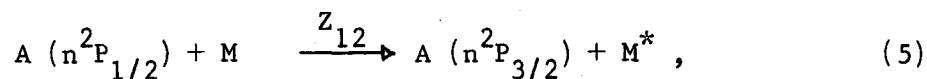
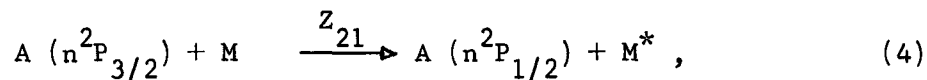
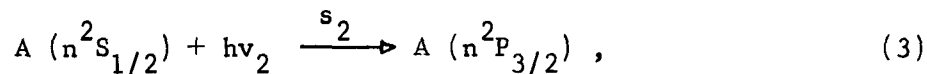


Fig. 1. Energy levels involved in sensitized fluorescence and in the quenching of alkali metal resonance radiation induced in collisions with molecules.

\* The  $D_1$  and  $D_2$  components are defined, by analogy with the Fraunhofer sodium D-lines, as the components of the alkali resonance doublet arising from the  $^2S_{1/2} \rightarrow ^2P_{1/2}$  and  $^2S_{1/2} \rightarrow ^2P_{3/2}$  transitions, respectively.

The various interactions between an alkali atom A and a diatomic molecule M may be represented by the following equations:



where  $n$  is the principal quantum number of the atomic state,  $s_2$  is the number of alkali atoms excited per second from the  $n^2S_{1/2}$  state to the  $n^2P_{3/2}$  state, and  $\tau_1$  and  $\tau_2$  are the mean lifetimes of the  $n^2P_{1/2}$  and  $n^2P_{3/2}$  states respectively.  $Z_{21}$ ,  $Z_{12}$ ,  $Z_{20}$ , and  $Z_{10}$  are the collision numbers for the processes designated in Fig. 1, defined as the numbers of collisions per excited alkali atom per second, leading to the appropriate excitation transfer process. M is a ground state diatomic molecule and  $M^*$  a molecule which, having participated in an inelastic collision, has become modified in its content of translational, vibrational, and rotational energy.

Collisional mixing in the  $^2P$  state due to alkali-alkali collisions has been neglected since the ratio of sensitized to resonance fluorescent intensities due to such collisions is of the order of  $10^{-6}$

to  $10^{-7}$  at the vapor pressures used in these experiments ( $10^{-6}$  Torr) and does not contribute significantly to the observed sensitized fluorescence<sup>20,21</sup>.

Assuming that the vapor-gas mixture exists in a state of dynamic equilibrium involving only continuous optical excitation of the  $A(n^2P_{3/2})$  state by means of  $D_2$  radiation, spontaneous decay, and the various binary collisional processes, Eqs. (3) - (9) may be combined to give the following rate equations:

$$\frac{d N(n^2P_{3/2})}{dt} = s_2 + N(n^2P_{1/2})Z_{12} - N(n^2P_{3/2})[(\tau_2)^{-1} + Z_{21} + Z_{20}] = 0, \quad (10)$$

$$\frac{d N(n^2P_{1/2})}{dt} = N(n^2P_{3/2})Z_{21} - N(n^2P_{1/2})[(\tau_1)^{-1} + Z_{12} + Z_{10}] = 0, \quad (11)$$

where, for example,  $N(n^2P_{1/2})$  denotes the density of alkali atoms in the  $n^2P_{1/2}$  state. Two additional rate equations, similar to Eqs. (10) and (11), may be obtained by considering the case of excitation with the  $D_1$  component of the resonance doublet.

The  $D_2$  fluorescence emitted by the vapor-gas mixture is a constant fraction (depending on geometry and the polarization of the fluorescence), say  $\epsilon$ , of the total energy emitted by the  $N(n^2P_{3/2})$  excited atoms, therefore, the intensity of the  $D_2$  component in the presence of a foreign gas is:

$$I(D_2) = \epsilon \gamma_2 h\nu_2 (\tau_2)^{-1} N(n^2P_{3/2}), \quad (12)$$

where  $\gamma_2$  is the response of the detecting system to  $D_2$  radiation of frequency  $\nu_2$ , and  $h$  is Planck's constant. The intensity of the  $D_2$  component in the absence of foreign gas is given by:

$$I_0(D_2) = \epsilon \gamma_2 h\nu_2 (\tau_2)^{-1} N_0(n^2P_{3/2}). \quad (13)$$

In a steady state involving no collision induced transitions  $(\tau_2)^{-1}N_0(n^2P_{3/2})$  equals the rate at which  $n^2P_{3/2}$  excited atoms are formed; that is,  $s_2$ , which depends on the incident and absorption  $D_2$  line profiles as well as the incident geometry.

If the atom-molecule collisions do not alter either the polarization of the resonance fluorescence ( $\epsilon = \text{constant}$ ) or the absorption line ( $s_2 = \text{constant}$ ), we can use Eqs. (10) - (13), and their analogues for  $D_1$  excitation, to derive expressions for the change in the intensity of the resonance fluorescence due to the mixing and quenching collisions.

In the case of excitation with the  $D_2$  component:

$$(I_o/I)_2 = 1 + \tau_2 Z_{20} + \tau_2 Z_{21} - (\tau_1 \tau_2 Z_{12} Z_{21}) / (1 + \tau_1 Z_{10} + \tau_1 Z_{21}) . \quad (14)$$

In the case of excitation with the  $D_1$  component:

$$(I_o/I)_1 = 1 + \tau_1 Z_{10} + \tau_1 Z_{12} - (\tau_1 \tau_2 Z_{12} Z_{21}) / (1 + \tau_2 Z_{20} + \tau_2 Z_{21}) . \quad (15)$$

$(I_o/I)_2$  is the ratio of the resonance fluorescent intensity (of wavelength appropriate to  $D_2$ ) observed in the absence of foreign gas to the intensity observed from the vapor gas mixture. When there is no  $^2P$  mixing ( $Z_{12} = Z_{21} = 0$ ), Eqs. (14) and (15) reduce to the usual Stern-Volmer form describing quenching in a two-state system:

$$(I_o/I) = 1 + \tau Z^{22}.$$

If both resonance and sensitized fluorescence is observed in the fluorescent light from the vapor-gas mixture, we define the ratio of their intensities as:

$$\eta_1 = I(D_1)/I(D_2) , \quad \eta_2 = I(D_2)/I(D_1) , \quad (16)$$

where the component appearing in the denominators is, in each case,

the same as that used in the exciting light. Equations (11) and (12), and their analogues for  $D_1$  excitation, can be used in conjunction with Eq. (16) to derive expressions for the  $^2P$  mixing collision numbers.

When  $D_2$  is used as the exciting light:

$$Z_{21} = (\tau_2)^{-1} \eta_1 (1 + \tau_1 Z_{10} + \tau_1 Z_{12}) , \quad (17)$$

and when  $D_1$  is used:

$$Z_{12} = (\tau_1)^{-1} \eta_2 (1 + \tau_2 Z_{20} + \tau_2 Z_{21}) . \quad (18)$$

Equations (17) and (18) can then be solved for  $Z_{21}$  and  $Z_{12}$ .

In the case of excitation with the  $D_2$  component:

$$Z_{21} = A + BZ_{10} + CZ_{20} . \quad (19)$$

In the case of excitation with the  $D_1$  component:

$$Z_{12} = D + EZ_{20} + CZ_{10} . \quad (20)$$

A, B, C, D and E are constants at any given gas pressure:

$$\begin{aligned} A &= (\tau_2)^{-1} \eta_1 (1 + \eta_2)/(1 - \eta_1 \eta_2) , \\ B &= \tau_1 \eta_1 (\tau_2)^{-1}/(1 - \eta_1 \eta_2) , \\ C &= \eta_1 \eta_2/(1 - \eta_1 \eta_2) , \\ D &= (\tau_1)^{-1} \eta_2 (1 + \eta_1)/(1 - \eta_1 \eta_2) , \\ E &= \tau_2 \eta_2 (\tau_1)^{-1}/(1 - \eta_1 \eta_2) . \end{aligned} \quad (21)$$

When quenching is negligible, Eqs. (19) and (20) are reduced to a more straightforward form representing  $^2P$  mixing;  $Z_{21} = A$  and  $Z_{12} = D^{23}$ .

Equations (14), (15), (19) and (20) provide the connection between the experimental observations ( $I_o/I$  and  $\eta$ ) and the collision numbers  $Z_{ab}$  which, for any given process  $a \rightarrow b$ , may be directly related, by analogy with the gas kinetic cross section, to the total effective

cross section  $Q_{ab}$  for the corresponding inelastic collision:

$$Z_{ab} = N(M) V_r Q_{ab} . \quad (22)$$

$V_r$ , the average relative velocity of the colliding partners, is given by the equation:

$$V_r = (8kT/\pi\mu)^{1/2} , \quad (23)$$

where  $k$  is the Boltzmann constant,  $T$  is the absolute temperature, and  $\mu$  is the reduced mass. Equation (22) indicates that at constant temperature, a plot of  $Z_{ab}$  against gas pressure should be linear and pass through the origin. The mixing cross sections  $Q_{12}$  and  $Q_{21}$  may be calculated point-for-point from low pressure data where quenching corrections are small or by iterative solutions of Eqs. (14), (15), (19) and (20) on a computer.

It has been implicitly assumed in the above treatment that there is no imprisonment of radiation. If resonance radiation is trapped, the effective lifetimes of the  $^2P$  levels are no longer equal to their mean lifetimes, which results in spurious values of the cross sections.

### III. DESCRIPTION OF THE APPARATUS

A typical arrangement of the apparatus used to study mixing and quenching collisions in potassium and cesium vapors is shown in Fig. 2. The alkali resonance doublet from a spectral lamp was separated by a monochromator in series with an interference filter. The monochromatic beam was then split into two parts: one was condensed into a fluorescence tube containing pure alkali vapor and the other into a similar tube containing a vapor-gas mixture. The fluorescent light from the latter tube was again resolved into its two spectral components by two interference filters in series and was focused onto the cathode

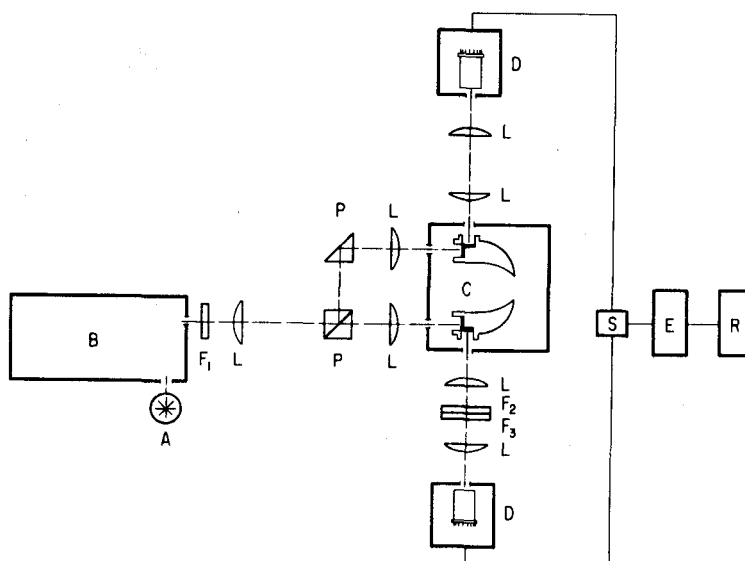


Fig. 2. Schematic diagram of apparatus. A, spectral lamp; B, monochromator; C, oven with fluorescence tubes; D, photomultiplier tubes; E, electrometer; R, recorder; S, coaxial switch;  $F_{1-3}$ , interference filters; L, lenses; P, prisms.

of a cooled photomultiplier. A second similar photomultiplier served to detect the total fluorescence from the tube containing pure alkali vapor. The output signals of both photomultipliers were directed, through a coaxial switch, to a picoammeter and registered with a strip chart recorder.

The light sources used in the experiments were commercial Osram lamps. To minimize self-reversal and keep the emission lines narrow, the lamps were operated at the lowest possible currents compatible with stability. The half-widths of the potassium lines were  $0.2 \text{ cm}^{-1}$  and  $0.3 \text{ cm}^{-1}$  for the  $D_1$  and  $D_2$  lines respectively<sup>24</sup>, and those of the corresponding cesium lines were  $0.1 \text{ cm}^{-1}$  and  $0.2 \text{ cm}^{-1}$ <sup>25</sup>.

The Bausch and Lomb monochromator was fitted with a 1200 line/mm grating blazed at  $7500 \text{ \AA}$  and giving a reciprocal dispersion of  $16 \text{ \AA/mm}$ . The entrance and exit slits were set at  $1.0 \times 10.0 \text{ mm}$  as a good compromise between intensity and resolution. With an appropriate Spectrolab interference filter in series, a beam purity of 1 part in  $10^5$  was obtained for the potassium lines. For cesium, a Schott interference-absorption filter gave further resolution and blocked second order grating transmissions. The resulting purity was 1 part in  $10^6$ . The  $D_1$  and  $D_2$  lines present in the fluorescent light from the vapor-gas mixture were resolved by two Spectrolab interference filters in series, whose transmissions and rejections were measured in situ. The potassium filters gave a spectral purity of about  $1:10^6$  and the cesium filters, a purity better than  $1:10^7$ .

The design of the fluorescence tubes, shown in Fig. 3, kept

reabsorption of resonance radiation to an absolute minimum by limiting the distance through which the exciting and fluorescent light had to travel through the absorbing vapor. The slit of the monochromator was focused in the corner formed by the entrance and exit windows and as a result, the maximum distance between either window and the observed region was about 1 mm. Reflections were suppressed by coating the tubes with Aquadag, a colloidal dispersion of graphite, and by forming the ends of the tubes into light traps.

Side arms, about 5 inches long and 3/4 inches in diameter, each contained about 0.5 g of alkali metal. The temperatures of these reservoirs determined the alkali vapor pressure in the tubes. Although, with such long side arms, it would be expected that the vapor pressure in the tubes should be lower than that predicted by the Taylor-Langmuir

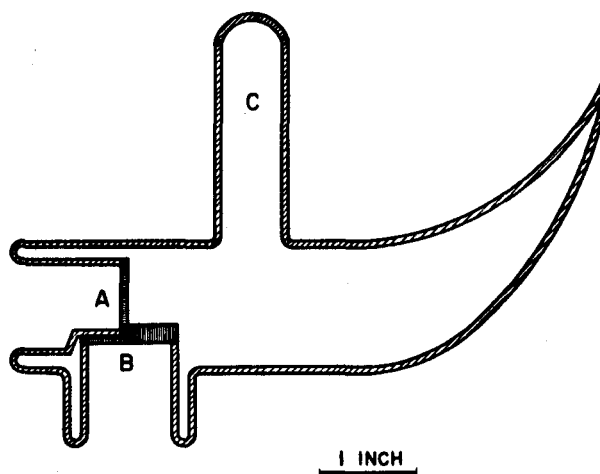


Fig. 3. The fluorescence tube. A, entrance window; B, exit window; C, side arm.

formula<sup>26</sup>, this was not an important consideration since, during the experiments, the vapor pressure was kept below  $2 \times 10^{-6}$  Torr while trapping of potassium and cesium resonance radiation becomes noticeable

only around  $1 - 2 \times 10^{-5}$  Torr<sup>20,21</sup>. With these low vapor pressures and restricted optical path lengths in the tubes, radiation trapping effects could be safely ignored.

Each fluorescence tube was connected to a vacuum and gas handling system by a 0.2 cm diameter capillary which successfully prevented migration of alkali vapor out of the tubes. Both tubes were mounted in a common double walled oven constructed of magnesium plate and transite board with fiber-glass insulation between the walls. Four General Electric strip heaters supplied from a Powerstat autotransformer kept the temperatures of the fluorescence tubes equal and constant within  $\pm 1^{\circ}\text{C}$  over long periods of time. The side arms of the tubes extended through the bottom of the main oven into separate smaller ovens constructed of brass pipes wound with copper tubing and insulated with asbestos rope. Water circulating through the copper coils from a Jena Ultrathermostat kept the temperatures of these ovens equal and constant to within  $\pm 0.2^{\circ}\text{C}$ . All temperatures were measured with calibrated copper-constantan thermocouples located at various points on the fluorescence tubes and side arms.

Vacuum was produced in the glass system by an Edwards EO-2 diffusion pump which was equipped with a cold trap containing a copper foil getter, and was backed with an ES-35 rotary pump. The lowest pressures that could be repeatedly obtained were about  $5 \times 10^{-8}$  Torr, but during an experimental run,  $1 \times 10^{-7}$  Torr was considered adequate. Vacuum measurements were carried out with a GIC-110A CEC ionization gauge with a GIC-016 ion gauge head ( $10^{-3} - 10^{-8}$  Torr), and a 3294B LKB

Autovac gauge with a Pirani head ( $10^2 - 10^{-3}$  Torr). Molecular gas pressures were roughly measured with an Edwards 8/2 Pirani gauge ( $1 - 10^{-3}$  Torr) with a G5B-2 Pirani head and then more accurately with a liquid-air trapped CVC McLeod gauge, type GM-100A, ( $10 - 10^{-3}$  Torr). The reproducibility of the McLeod measurements was better than three per cent.

The photomultipliers were 16-stage ITT FW-118G tubes with S-1 photocathodes 3 mm in diameter. The 1.5 kV operating voltage was supplied by a 413-C Fluke regulated power supply and resistive divider chains distributed about 80 volts to each dynode. Cooled to liquid nitrogen temperatures in cryostats, the photomultipliers had dark currents of the order of  $10^{-13}$  amperes. A model 417 Keithley High Speed Picoammeter followed by a Daystrom-Weston 10 mV strip chart recorder was capable of measuring signals down to  $1 \times 10^{-13}$  amperes.

The quantum efficiencies of the S-1 surface for  $D_1$  and  $D_2$  radiation ( $\gamma_1$  and  $\gamma_2$  respectively) were equal for the potassium resonance lines but for the cesium lines which are further apart:

$$\gamma_1 = 0.31 \text{ per cent} \quad \text{and} \quad \gamma_2 = 0.35 \text{ per cent.}$$

#### IV. EXPERIMENTAL PROCEDURE

After baking each fluorescence tube for 48 h at 200°C and at a vacuum of  $6 \times 10^{-8}$  Torr, about 0.5 g of alkali metal was distilled under vacuum into the side arms which were then sealed off. (Cesium, 99.99 per cent pure, and potassium, 99.95 per cent pure, were supplied in glass ampules by the A. D. McKay Company of New York.) When all the metal had migrated to the bases of the side arms, the temperature of the tubes was stabilized at about 15°C above the temperature of the metal reservoirs. Finally, after optimizing the optical alignment and measuring the filter transmissions, a very small amount of gas was admitted into one of the tubes through its capillary while the other remained connected to the vacuum system.

Linde M.S.C. grade H<sub>2</sub> and N<sub>2</sub> (nominal purity 99.99 per cent), HD (99 per cent) supplied by Stohler Isotope Chemicals, and Matheson C.P. grade D<sub>2</sub> (99.5 per cent), were used in the experiments. The gases were dried by slow passage through a liquid-nitrogen trap and were further purified by gettering them with hot potassium or cesium for several days.

When a component of the alkali resonance doublet was made incident on both tubes, it was found that the ratio of the resonance fluorescent intensities from the two tubes was independent of the shape and intensity of the incident line, which could be varied by changing the operating current of the Osram lamp. The ratio did

slightly depend on the alkali vapor pressure because of small differences between the geometries of the two tubes. Since, however, the temperatures of the side arms were quite stable, no significant error arose from this effect. Therefore, in the absence of absorption line broadening, it was possible to obtain the intensity of the resonance fluorescence in the gas-filled tube, which would have been produced in the absence of gas, by measuring the intensity of the fluorescence emerging from the tube containing the pure vapor and multiplying it by a previously determined conversion factor. Using this method to measure  $(I_0/I)$  it was possible to detect a three per cent decrease in the resonance fluorescent intensity.

The intensity ratios  $\eta$ , appropriate to the  $^2P_{1/2} - ^2P_{3/2}$  excitation transfer, were determined by measuring directly the relative intensities of the two resonance components present in the fluorescent light emerging from the tube containing the vapor-gas mixture.

All McLeod gauge pressure measurements were corrected for molecular transpiration which took place in the capillary connecting the gas handling system to the fluorescence tube when the mean free path of the gas molecules was greater than the diameter of the capillary. Under these circumstances the ratio of the pressure in the tube,  $P_t$ , to

the pressure measured at the McLeod gauge,  $P_m$ , is given by:

$$P_t/P_m = (T_t/T_m)^{1/2}, \quad (24)$$

where  $T_t$  and  $T_m$  are the absolute temperatures at the tube and gauge, respectively. This correction amounted to, at most, ten per cent and was usually applicable only at pressures below 0.05 Torr. No corrections were made for the streaming of mercury vapor toward the cold trap<sup>27</sup> or for the pumping effect of the McLeod gauge<sup>28</sup> since the errors involved appear to be small in the pressure range  $10^{-2}$  - 2 Torr.

In the experiments involving potassium both fluorescence tubes were kept at  $90 \pm 1^\circ\text{C}$  and their side arms at  $70.5 \pm 0.2^\circ\text{C}$ , whereas in the cesium experiments the temperatures were  $42 \pm 1^\circ\text{C}$  and  $30.5 \pm 0.2^\circ\text{C}$ , respectively. The pertinent information regarding the D lines of the two alkalis is listed in Table I.

TABLE I

The D-Lines of Potassium and Cesium

	$D_1$ (Å)	$D_2$ (Å)	Mean Lifetimes of the $^2P$ States ( $10^{-8}$ sec.)
K	7699	7665	$\tau_1 = \tau_2 = 2.7^a$
Cs	8944	8521	$\tau_1 = 3.8^b$ $\tau_2 = 3.3$

<sup>a</sup> Reference 29

<sup>b</sup> Reference 30

## V. SENSITIZED FLUORESCENCE AND QUENCHING IN MIXTURES

### OF POTASSIUM WITH $N_2$ , $H_2$ , HD AND $D_2$

#### A. The K - $N_2$ Collision Cross Sections

The intensity ratios  $\eta$ , arising from the collisional  $^2P_{1/2} \text{ --- } ^2P_{3/2}$  excitation transfer, are shown as functions of  $N_2$  pressure in Fig. 4, and the intensity ratios  $I_0/I$  are similarly represented in Fig. 5. (The numerical data for all the experiments are collected in Appendix A.) The decrease in the resonance fluorescent intensity with increasing gas pressure, shown in Fig. 5, is due partly to real quenching (radiationless decay of  $K^*$  to the ground

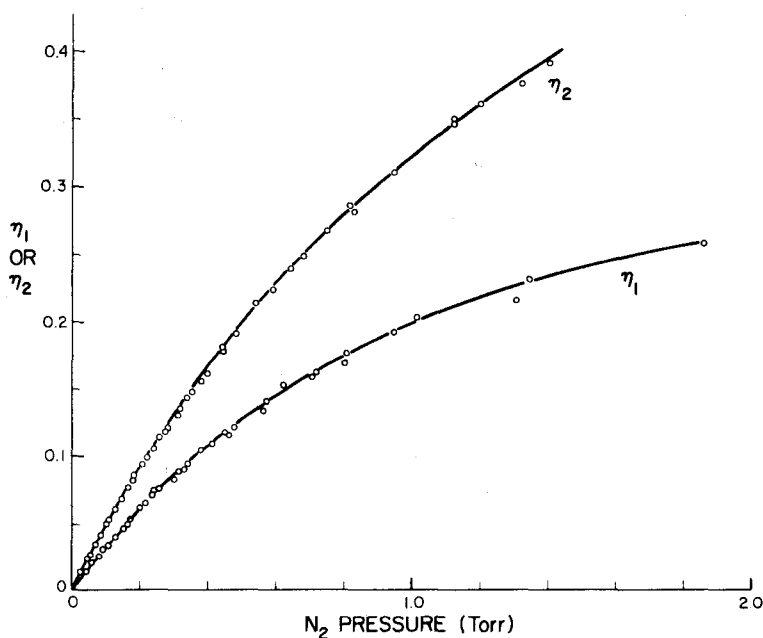


Fig. 4. Plots of intensity ratios  $\eta_1$  and  $\eta_2$  against  $N_2$  pressure showing sensitized fluorescence in potassium.

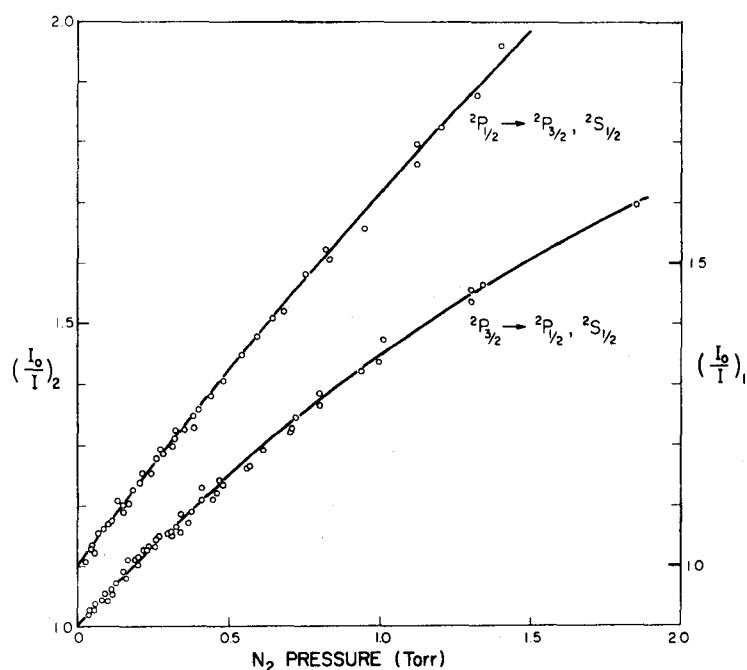


Fig. 5. Plots of intensity ratios  $I_0/I$  against  $N_2$  pressure showing collisional de-excitation involving both quenching and  ${}^2P_{1/2} - {}^2P_{3/2}$  mixing processes.

state) but is caused to an even greater extent by the  ${}^2P$  mixing process which gives rise to the curvatures in the plots, as would be expected from Eqs. (14) and (15). The slopes of the graphs are also affected by two additional factors. With the relatively broad lines used for the excitation of the fluorescence, pressure broadening in the fluorescing vapor-gas mixture would increase the absorption efficiency and hence decrease the slopes at higher gas pressures. The effects of pressure broadening (and shifting) of the potassium absorption lines should, however, be very small below a few Torr of  $N_2$ <sup>31</sup>. More importantly, traces of chemically reactive impurities in the gas would tend to decrease the potassium atom density in the fluorescence tube and thus increase the slopes of the curves.

The collision numbers  $Z_{10}$  for  ${}^2P_{1/2} \longrightarrow {}^2S_{1/2}$  quenching and  $Z_{12}$  for  ${}^2P_{1/2} \longrightarrow {}^2P_{3/2}$  excitation transfer are plotted against  $N_2$  pressure in Fig. 6. The plots of  $Z_{20}$  and  $Z_{21}$ , which are easily obtained from the results contained in Figs. 4 and 5, appear similar. The values of  $Z_{12}$  represented by crosses were calculated point-for-point from the  $\eta$  values in Fig. 4, using only the first term in Eq. (20). This treatment neglects the quenching effects that cause the curvature which sets in around 0.2 Torr. The circles represent the values of the collision numbers  $Z_{12}$  (and  $Z_{10}$ ) obtained by iterative solutions of Eqs. (14), (15), (19) and (20) on an IBM 1620 computer (see Appendix B), using all the data from Figs. 4 and 5. The collision numbers thus obtained lie on the broken straight line extrapolated from the low pressure values of  $Z_{12}$ , which are almost completely unaffected by quenching and which are considered to be the most reliable data obtained in these experiments. The mixing cross sections  $Q_{12}$  and  $Q_{21}$ , obtained from point-for-point calculations using the low pressure data below 0.2 Torr, are given in Table II. It is noteworthy that least squares analyses of the  $Z_{12}$  (and  $Z_{21}$ ) values represented by the circles in Fig. 6 yielded mixing cross sections within five per cent of the values given in the table.

The quenching cross sections  $Q_{10}$  and  $Q_{20}$ , which are presented in Table III, were calculated in two ways. They were obtained directly from plots of  $Z_{10}$  (and  $Z_{20}$ ) against  $N_2$  pressure, and also from the differences between the solid and broken curves representing  $Z_{12}$  (or  $Z_{21}$ ) as outlined in Appendix C. The two methods yielded results which were

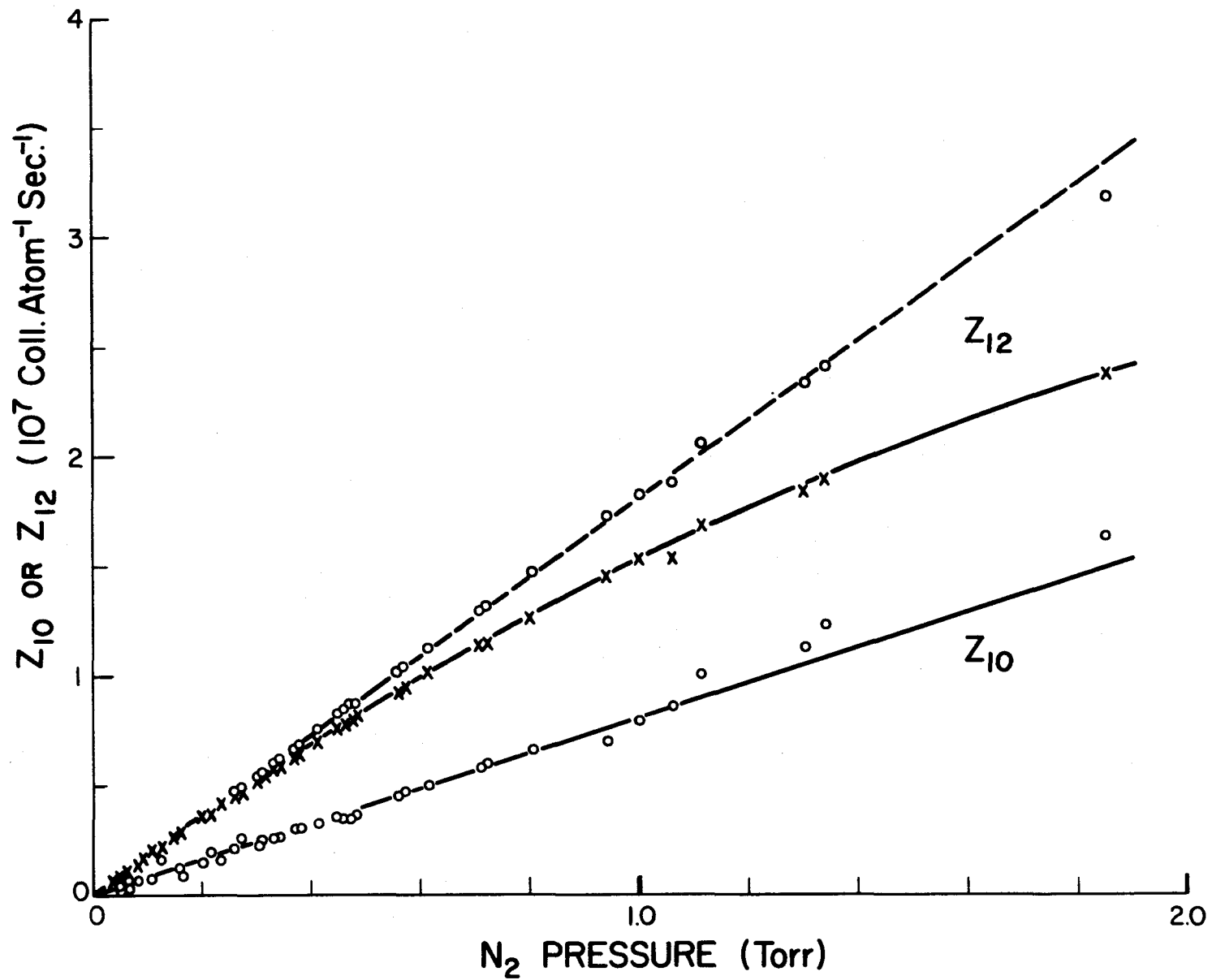


Fig. 6. Plots of collision numbers  $Z_{10}$  and  $Z_{12}$  against  $N_2$  pressure. x, results uncorrected for quenching; o, results obtained from iterative solutions of Eqs. (14), (15), (19) and (20). The broken line has been extrapolated from low pressure data.

within twenty per cent of one another but it is believed that the latter method is more reliable since the measurements of  $\eta$  involve only excited atoms and are unaffected by either pressure broadening or reactive impurities which combine with ground state potassium atoms. The ratios  $I_0/I$  which must be used in the first method are strongly affected by such impurities and, when quenching is slight, which tends to be the case at the low gas pressures used, an error of just a few per cent in the value of  $I_0/I$  introduces an uncertainty of 30 - 50 per cent into the quenching cross sections.

#### B. The K - H<sub>2</sub>, K - HD and K - D<sub>2</sub> Collision Cross Sections

The ratios  $\eta$  of sensitized-to-resonance fluorescent intensities are shown as functions of the gas pressures in Figs. 7 and 8, and the ratios  $I_0/I$  are plotted against D<sub>2</sub> pressure in Fig. 9 which is typical of all the remaining systems. The upward curvature in the  $(I_0/I)_1$  graph is attributed to chemically reactive impurities in the deuterium. In the case of the  $(I_0/I)_2$  curve, the effect of these impurities is outweighed by the reverse  $^2P_{1/2} \longrightarrow ^2P_{3/2}$  process which has a relatively large probability because of the greater statistical weight of the  $^2P_{3/2}$  state.

Figure 10 shows plots of the collision numbers  $Z_{12}$  and  $Z_{10}$  as functions of D<sub>2</sub> pressure, and is again representative of the collision numbers in all the mixtures with H<sub>2</sub>, HD and D<sub>2</sub>. As in the K - N<sub>2</sub> mixture, the crosses were obtained from the  $\eta$  values using only the first term in Eq. (20). In the present case, however, they do fall on

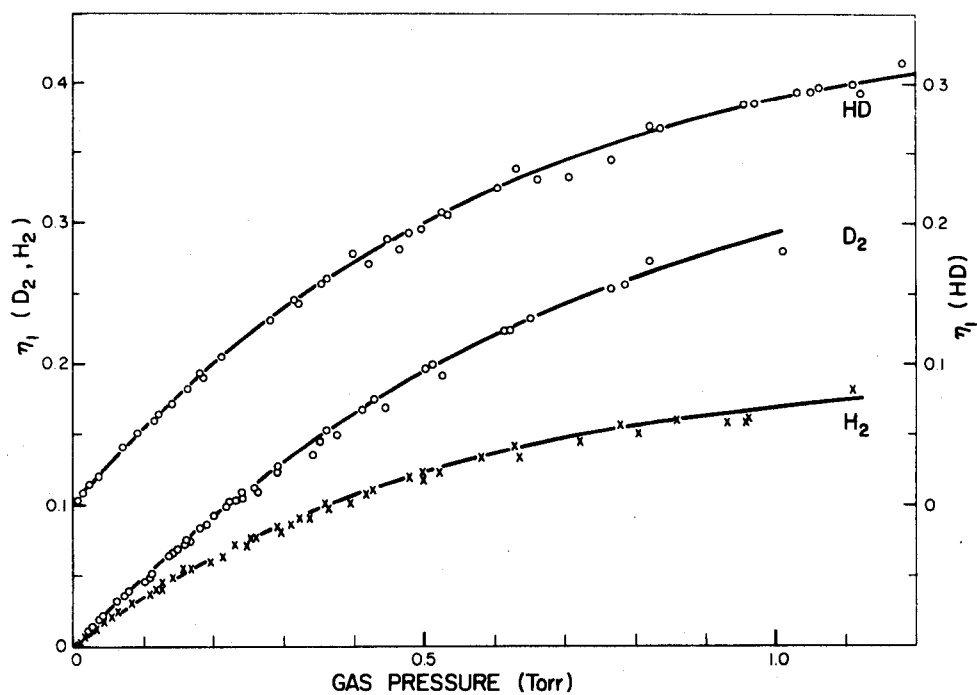


Fig. 7. Plots of intensity ratios  $\eta_1$  against  $H_2$ , HD and  $D_2$  pressures.

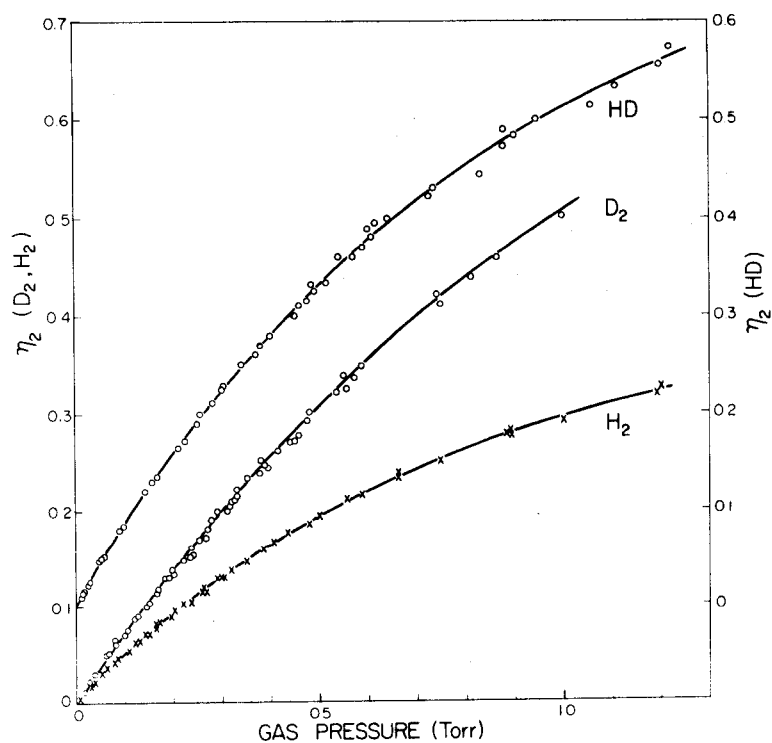


Fig. 8. Plots of intensity ratios  $\eta_2$  against  $H_2$ , HD and  $D_2$  pressures.

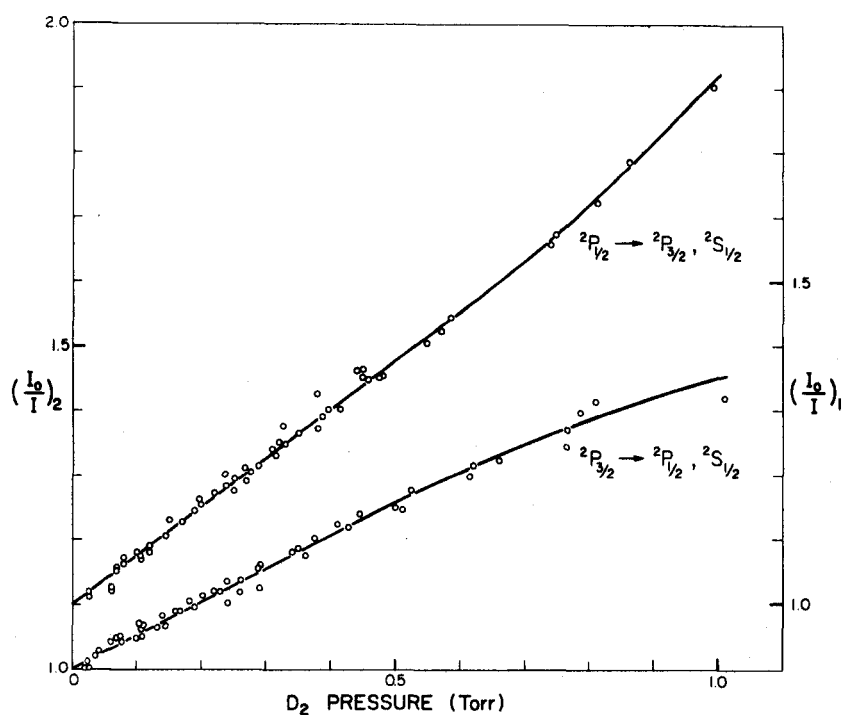


Fig. 9. Plots of intensity ratios  $I_0/I$  against  $D_2$  pressure.

the broken line extrapolated from the low pressure data, indicating a much smaller amount of quenching. The scatter of the  $Z_{10}$  points and the non-linearity of the graph are probably caused by the trace impurities in the deuterium which also cause an upward trend in the  $Z_{12}$  values obtained from iterative solutions (circles). The excitation transfer cross sections  $Q_{12}$  and  $Q_{21}$  and the quenching cross sections  $Q_{10}$  and  $Q_{20}$ , which were calculated in the same manner as for the K -  $N_2$  collisions, are listed in Tables II and III, respectively.

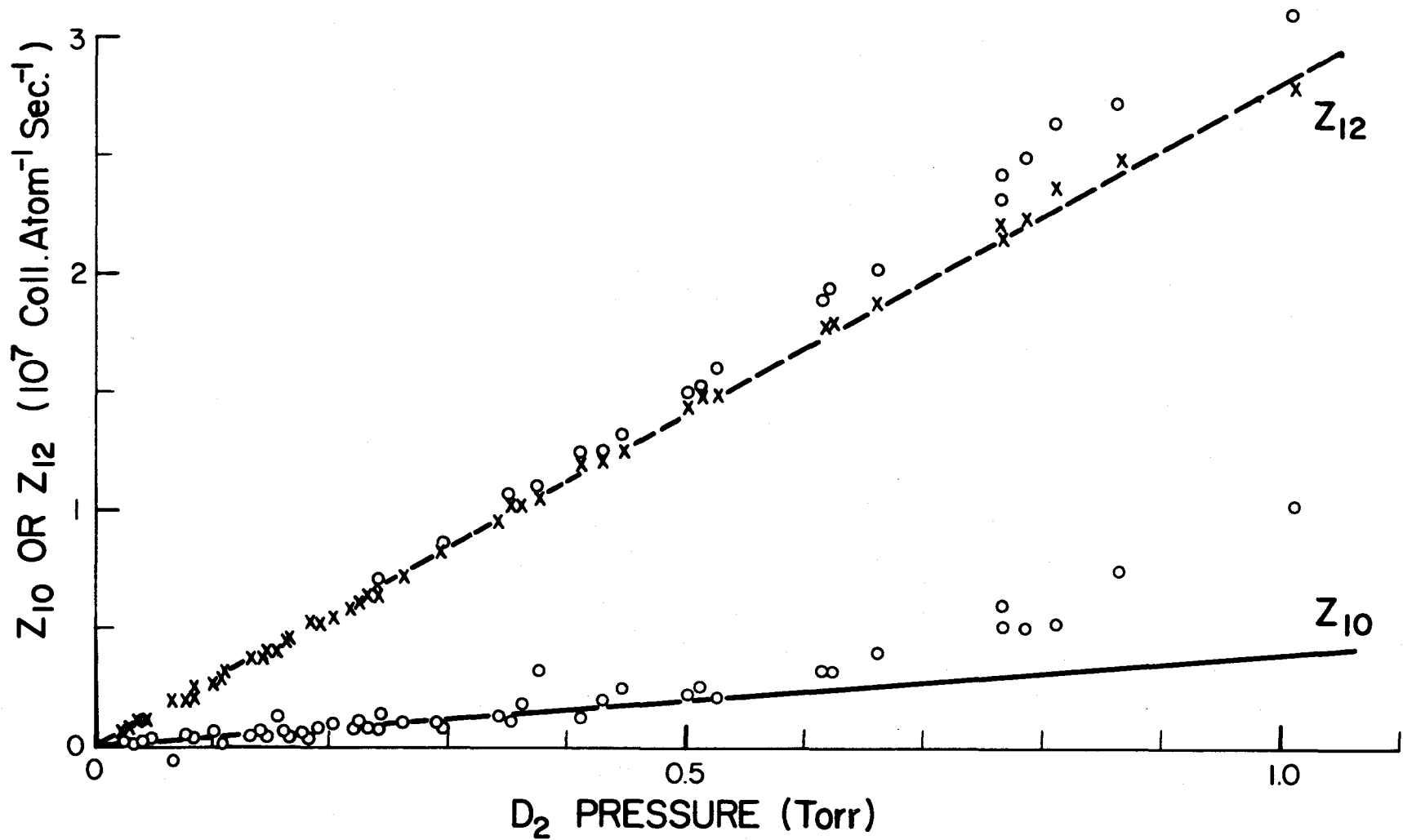


Fig. 10. Plots of collision numbers  $Z_{10}$  and  $Z_{12}$  against  $D_2$  pressure. x, results uncorrected for quenching; o, results obtained from iterative solutions of Eqs. (14), (15), (19) and (20). The broken line has been extrapolated from low pressure data.

TABLE II

Cross Sections for Excitation Transfer in K - Molecule Collisions

Collision Partners	$Q_{12} (4^2P_{1/2} \rightarrow 4^2P_{3/2})$ ( $\text{\AA}^2$ )	$Q_{21} (4^2P_{1/2} \leftarrow 4^2P_{3/2})$ ( $\text{\AA}^2$ )	$\frac{Q_{12}}{Q_{21}}$
K - N <sub>2</sub>	99.7	66.0	1.51
K - H <sub>2</sub>	75.6	53.2	1.42
K - D <sub>2</sub>	72.2	50.4	1.44
K - HD	74.0	48.7	1.52

TABLE III

Cross Sections for Quenching in K - Molecule Collisions

Collision Partners	$Q_{10} (4^2S_{1/2} \leftarrow 4^2P_{1/2})$ ( $\text{\AA}^2$ )	$Q_{20} (4^2S_{1/2} \leftarrow 4^2P_{3/2})$ ( $\text{\AA}^2$ )
K - N <sub>2</sub>	35 ± 7	39 ± 8
K - H <sub>2</sub>	7 ± 3	4 ± 1.5
K - D <sub>2</sub>	2 ± 1	1 ± 0.5
K - HD	11 ± 4	14 ± 3

## VI. SENSITIZED FLUORESCENCE AND QUENCHING IN MIXTURES OF CESIUM

WITH  $N_2$ ,  $H_2$ , HD AND  $D_2$

It was originally thought that, in order to arrive at the  $^2P$  mixing cross sections  $Q_{ab}$ , it would be necessary to apply corrections for quenching and, therefore, to measure the quenching cross sections  $Q_{bo}$ . The experimental results obtained for the K -  $N_2$  collisions, described in Chapter V, suggest otherwise. In systems in which  $Q_{ab} > Q_{bo}$  the corrections are superfluous at relatively low pressures and may even render the mixing cross sections less precise if the impurity content of the quenching gas is high (cf. the K -  $D_2$  results). Even when  $Q_{ab} < Q_{bo}$  the mixing efficiencies may still be accurately determined without prior knowledge of the quenching cross sections since the de-excitation effects enter Eqs. (19) and (20) only as second order corrections. For these reasons the cesium experiments were conducted with only one fluorescence tube and no attempt was made to measure the quenching cross sections directly.

The measured ratios of sensitized-to-resonance fluorescent intensities,  $\eta'$ , were multiplied by the appropriate frequency ratio of the  $D_1$  and  $D_2$  cesium lines and the quantum efficiency ratio of the photomultiplier for these lines in accordance with Eq. (12):  $\eta_1 = \eta'_1 \times 1.19$ ,  $\eta_2 = \eta'_2 \times 0.84$ . The corrected  $\eta$ -values corresponding to  $^2P_{1/2} \text{ --- } ^2P_{3/2}$  excitation transfer in cesium are shown as a function of  $N_2$  pressure in Fig. 11 and as functions of  $H_2$ , HD and  $D_2$  pressures

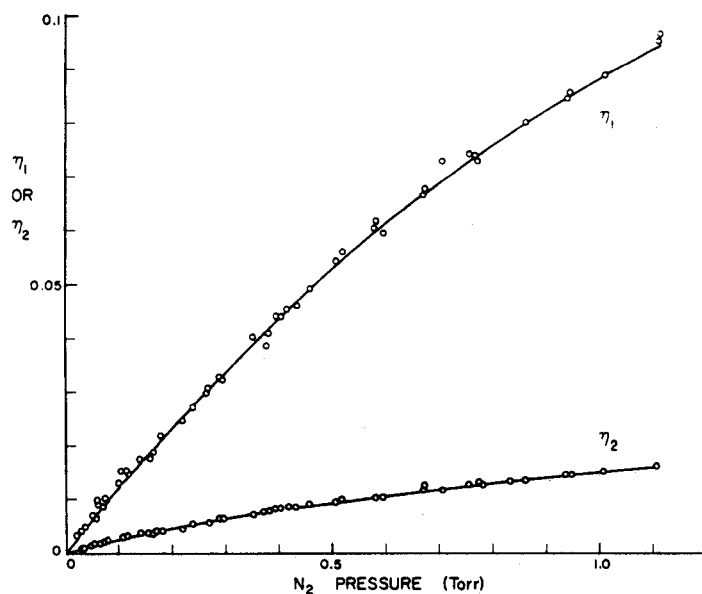


Fig. 11. Plots of intensity ratios  $\eta_1$  and  $\eta_2$  against  $N_2$  pressure showing sensitized fluorescence in cesium.

in Figs. 12 and 13.

The collision numbers  $Z_{12}$  and  $Z_{21}$  were calculated point-for-point from the data of Figs. 11 - 13 using only the first terms in Eqs. (19) and (20). The values for  $H_2$ , which are representative of all the results, are plotted against  $H_2$  pressure in Fig. 14. Here again the broken straight line has been extrapolated from the low pressure data where the collision numbers are linear with pressure. The mixing cross sections  $Q_{12}$  and  $Q_{21}$  and the quenching cross sections  $Q_{10}$  and  $Q_{20}$ , which were calculated as in Chapter V, are presented in Tables IV and V, respectively.

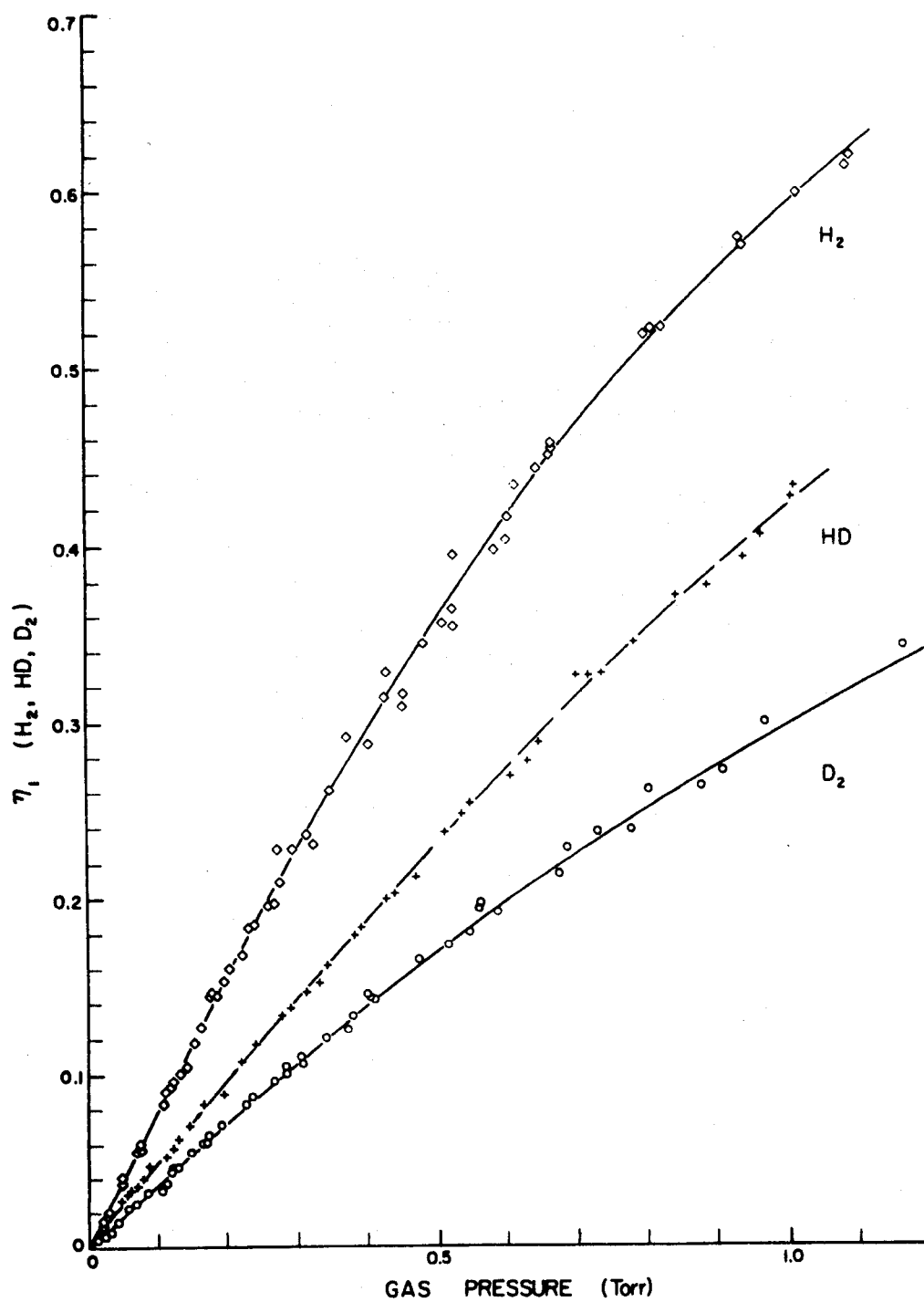


Fig. 12. Plots of intensity ratios  $\eta_1$  against H<sub>2</sub>, HD and D<sub>2</sub> pressures.

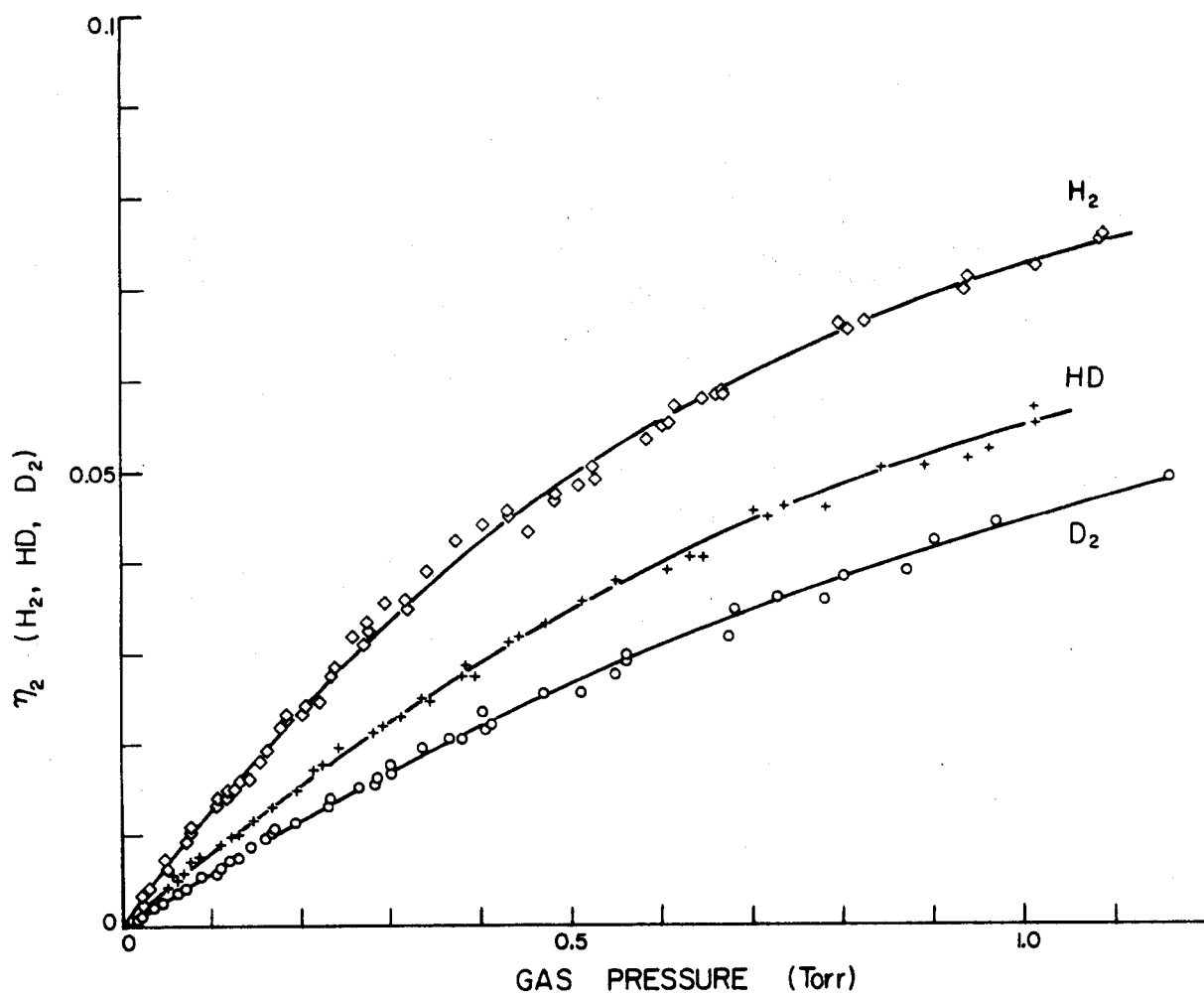


Fig. 13. Plots of intensity ratios  $\eta_2$  against H<sub>2</sub>, HD and D<sub>2</sub> pressures.

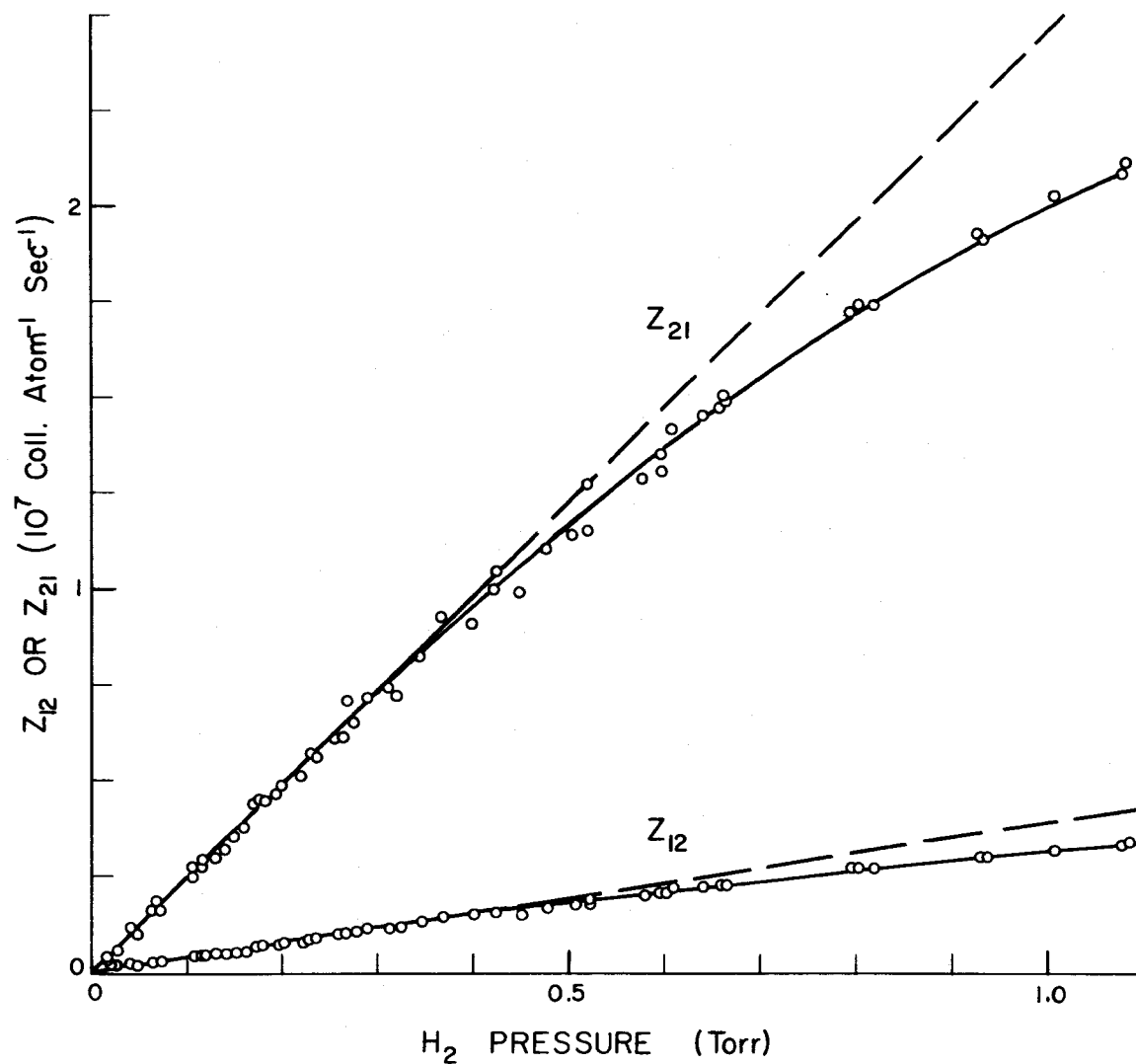


Fig. 14. Plots of collision numbers  $Z_{12}$  and  $Z_{21}$  against  $H_2$  pressure. The broken line has been extrapolated from low pressure data.

TABLE IV

## Cross Sections for Excitation Transfer in Cs - Molecule Collisions

Collision Partners	$Q_{12} (6^2P_{1/2} \rightarrow 6^2P_{3/2})$ ( $\text{\AA}^2$ )	$Q_{21} (6^2P_{1/2} \leftarrow 6^2P_{3/2})$ ( $\text{\AA}^2$ )	$\frac{Q_{12}}{Q_{21}}$
Cs - N <sub>2</sub>	4.7	25.2	0.186
Cs - H <sub>2</sub>	6.7	43.8	0.153
Cs - D <sub>2</sub>	4.2	27.8	0.151
Cs - HD	4.8	32.1	0.149

TABLE V

## Cross Sections for Quenching in Cs - Molecule Collisions

Collision Partners	$Q_{10} (6^2S_{1/2} \leftarrow 6^2P_{1/2})$ ( $\text{\AA}^2$ )	$Q_{20} (6^2S_{1/2} \leftarrow 6^2P_{3/2})$ ( $\text{\AA}^2$ )
Cs - N <sub>2</sub>	62 ± 19	100 ± 30
Cs - H <sub>2</sub>	7 ± 2	5 ± 2
Cs - D <sub>2</sub>	8 ± 3	7 ± 5
Cs - HD	4 ± 1	3 ± 2

## VII. DISCUSSION OF THE RESULTS

### A. Accuracy of the Results

The statistical uncertainty in the mixing cross sections  $Q_{12}$  and  $Q_{21}$  was smaller than  $\pm 5$  per cent for all the mixtures. The systematic errors introduced by the filter transmissions, McLeod gauge readings and temperature measurements were estimated to be about 3 per cent each and the mean lifetimes of the potassium and cesium resonance states were considered accurate to 4 per cent. Taking account of all these error sources, the mixing cross sections are thought to be correct within 8 per cent.

The quenching cross sections  $Q_{10}$  and  $Q_{20}$ , which are a by-product of the excitation transfer studies, are not nearly as accurate as the mixing cross sections. The errors assigned to the values given in Tables III and V were estimated by using the upper and lower limits of  $Q_{12}$  and  $Q_{21}$  in the quenching cross section calculation.

The beam-splitting prism caused a 31 per cent polarization of the exciting light parallel to the direction of observation (horizontally polarized). With pure potassium vapor in the fluorescence tubes, the 7665 Å component of the resonance fluorescence was approximately 8 per cent polarized and the 7699 Å component was unpolarized, as expected. Depolarizing collisions were estimated to have increased the 7665 Å fluorescent intensity, emitted in the direction of observation,

by about 3 per cent<sup>32</sup> and would thus have introduced a further slight error into the potassium results. In the cesium experiments the beam splitter was not in place. With unpolarized light incident on the fluorescence tube the 8521 Å cesium fluorescence was 3 per cent polarized and the 8944 Å fluorescence unpolarized so that depolarizing collisions might increase the 8521 Å fluorescent intensity by less than 1 per cent.

#### B. The Quenching Cross Sections

The quenching cross sections for potassium - N<sub>2</sub>, H<sub>2</sub> and D<sub>2</sub> collisions are compared in Table VI with results obtained from investigations of flames<sup>7</sup>, photolysis of KI<sup>8</sup> and conventional intensity measurements<sup>9</sup>. It should be borne in mind that none of the other authors attempted to separate the two components of the potassium resonance doublet and that each of the quoted values should thus be expected to lie somewhere between our Q<sub>10</sub> and Q<sub>20</sub>. The agreement between our hydrogen and deuterium results with those of reference 9, which were obtained under similar conditions, is encouraging. It appears that the magnitudes of the quenching cross sections increase with decreasing velocity. Similar behaviour has been observed over limited velocity ranges in sodium quenching experiments<sup>7</sup>. The implication is that the quenching process is carried out with the expenditure of little or no additional energy.

With the possible exception of the Cs - N<sub>2</sub> system there seems to be no conspicuous difference between the two cross sections Q<sub>10</sub> and Q<sub>20</sub> for any particular gas. There is also no appreciable

TABLE VI

Reported Quenching Cross Sections for K - Molecule Collisions  
at Various Average Relative Velocities  $V_r$

Quenching Species	Reference	$V_r$ ( $10^5$ cm/sec.)	Cross Section ( $\text{\AA}^2$ )
$N_2$	8	1.62	10
$N_2$	7	1.58	18
$N_2$	7	1.51	19
$N_2$	8	1.31	21
$N_2$	8	0.91	20
$N_2$	This Investigation	0.69	$Q_{10} = 35$ $Q_{20} = 39$
-----			
$H_2$	7	4.81	3.4
$H_2$	7	4.53	3.7
$H_2$	This Investigation	2.00	$Q_{10} = 7$ $Q_{20} = 4$
$H_2$	9	1.96	6.2
-----			
$D_2$	This Investigation	1.45	$Q_{10} = 2$ $Q_{20} = 1$
$D_2$	9	1.42	4.5

variation (within error) among the  $H_2$ ,  $D_2$  and HD cross sections for quenching of potassium or cesium resonance radiation. These two facts imply that resonant transfer of electronic to vibrational energy does not play a major role in determining the sizes of the quenching cross sections. The  $^2P$  cesium levels are at 11,181 and 11,735  $cm^{-1}$  while the potassium levels are at 12,989 and 13,047  $cm^{-1}$ . The  $v = 3$  level of  $H_2$ , for example, has an energy of 11,782  $cm^{-1}$ . If vibrational resonances involving these levels determined the quenching mechanism the cesium  $^2P$  states, and the  $^2P_{3/2}$  state in particular, should be quenched far more by hydrogen than the potassium states; this is, in fact, not the case.

These results are not inconsistent with the idea that quenching proceeds by way of an intermediate complex. As already noted, the role of such a complex in  $Na^* - H_2$  quenching collisions has been considered in detail by Magee and Ri<sup>16</sup> and Laidler<sup>17</sup>. In Magee and Ri's treatment the critical state of the complex corresponds to the top of the rotational energy barrier. The cross section for quenching is estimated by assuming that complexes with rotational energy below a specific value have during their lifetime a probability of transition to the ground state (by way of an ionic state) close to unity. Laidler relates the quenching cross section to that separation of  $Na^*$  and  $H_2$  which permits 'contact' between the excited and ionic ( $Na^+ + H_2^-$ ) potential energy surfaces. Both approaches require an extension of the H - H bond to allow formation of the ionic complex. Magee and Ri indicate that the quenching cross sections of potassium and cesium should be less than that of sodium whereas Laidler's treatment

suggests the opposite. Since recent determinations of the  $\text{Na}^* - \text{H}_2$  quenching cross section show it to be larger than the potassium and cesium cross sections<sup>33</sup>, Magee and Ri's interpretation seems to be preferred.

The quenching cross sections are smaller than the  $^2\text{P}$  mixing cross sections, the lone exception being that of  $\text{Cs}^* - \text{N}_2$  quenching. Thus the regions of the potential energy surfaces corresponding to the quenching and mixing transitions are probably well separated. There is also no conclusive evidence that either of the  $^2\text{P}_J$  levels is more susceptible to quenching than the other. It seems, therefore, that once the region responsible for the  $^2\text{P}_{1/2} - ^2\text{P}_{3/2}$  transitions has been passed, all the electronic molecular states of the excited intermediate complex ( $^2\Sigma^+$  and  $^2\pi$  for a linear complex) are equally likely to be populated so that it should make little difference which of the  $^2\text{P}_J$  levels had been originally excited. The  $\text{Cs} - \text{N}_2$  results are anomalous in that the mixing cross sections are smaller by about a factor of three than the quenching cross sections. Therefore if one of the  $^2\text{P}_J$  states were, in fact, more strongly quenched than the other, the effect should be detectable in this system. Although the large errors in the quenching cross sections reported here prohibit a meaningful conclusion on this point, the  $^2\text{P}_{3/2}$  state of cesium does seem to be more strongly quenched by  $\text{N}_2$ . It might be interesting to examine the  $\text{Cs}^* - \text{N}_2$  quenching reaction with a more accurate technique, such as the method of delayed coincidences described in reference 33, to see if this is indeed the case.

### C. The $^2P$ Mixing Cross Sections

The potassium-molecule  $^2P$  mixing cross sections  $Q_{12}$  and  $Q_{21}$  are of the same order of magnitude but slightly larger than the corresponding potassium-inert gas cross sections<sup>1</sup>. A similar relationship in the case of sodium-molecule collisions can be deduced from Lochte-Holtgreven's results. This suggests that the interaction which causes spin-orbit decoupling in an excited alkali atom is not appreciably stronger for nonpolar diatomic molecules than for inert gas atoms. The alkali-molecule interaction is probably a quadrupole-quadrupole type of interaction with an  $r^{-5}$  potential whereas the alkali-inert gas interaction has a van der Waals' potential varying as  $r^{-6}$  or faster<sup>34</sup>. The potassium  $Q_{21}$  mixing cross sections appear to exhibit a slight but distinct correlation with the molecular rotational levels. The somewhat larger K - N<sub>2</sub> cross sections may well be due to the fact that the (J = 6) — (J = 8) transition in N<sub>2</sub> has an energy of 60 cm<sup>-1</sup> while the energy defect,  $\Delta E$ , between the potassium resonance levels equals 58 cm<sup>-1</sup>. The cross sections for H<sub>2</sub>, D<sub>2</sub> and HD, none of which has rotational transitions in this energy range, are all smaller and are equal within experimental error. This latter point indicates that the interaction mechanism for  $^2P$  mixing is the same for these isotopic molecules, which might be expected because H<sub>2</sub>, D<sub>2</sub> and HD have similar electronic structures. The fact that the energy defect in potassium is less than  $kT$  (253 cm<sup>-1</sup>) would tend to minimize the effect of a resonance with the rotational transitions since, with the available excess of translational kinetic energy,  $^2P$  mixing would not depend exclusively on

a concurrent rotational transition taking place in the participating molecule. If such a resonant transfer occurred, a more pronounced effect would be expected in the cesium-molecule mixing collisions where the energy defect is two and one-half times larger than  $kT$ .

The cesium-molecule mixing cross sections are five orders of magnitude larger than the cesium-inert-gas mixing cross sections<sup>1</sup>. Such a large disparity between the mixing efficiencies of molecules and inert-gas atoms cannot be attributed to their different interaction potentials since no such vast difference in the mixing cross sections was observed in the potassium (or sodium) systems. The determining factor seems to be that the energy defect between the cesium  $^2P$  states, which equals  $554 \text{ cm}^{-1}$ , falls within the energy range of the molecular rotational levels. The rotational levels in  $N_2$  are altogether too closely spaced to permit any sharp resonance effect corresponding to a particular rotational transition. In  $H_2$ , however, the transition ( $J = 1$ ) — ( $J = 3$ ) has an energy of  $587 \text{ cm}^{-1}$ , close enough to the  $^2P$  energy defect to envisage the possibility of a resonance. Evidence in favor of such a resonance is provided by the fact that the  $Cs - H_2$   $Q_{21}$  cross section is larger than the corresponding  $Cs - N_2$  cross section whereas the opposite is true with the  $K - H_2$  and  $K - N_2$  systems. Additional support for a mechanism involving the rotational states is lent by the variation in the  $Cs - H_2$ ,  $D_2$  and  $HD$  mixing cross sections which, unlike the same cross sections in potassium, are not equal even within experimental error. Since the potassium results suggested that the alkali-molecule interaction potentials were similar for  $H_2$ ,  $D_2$  and

HD a rather strong dependence of the cesium mixing cross sections on the rotational structure of these molecules is indicated. Assuming that there are no potential curve crossings in the region responsible for mixing and that rotational transitions do occur in the mixing process, the magnitude of the  $Q_{21}$  cross section should be largely determined by the difference between the amount of energy released in the cesium  ${}^2P_{1/2} \leftarrow {}^2P_{3/2}$  transition and the energy that the colliding molecule may take up in a rotational transition. This energy difference,  $\delta E$ , would have to be given to or taken from the translational kinetic energy continuum and, according to Franck's rule<sup>35</sup>, the cross section for such a process,  $\sigma$ , should have the following dependence on the absolute value of  $\delta E$ :

$$\sigma \propto (\delta E)^{-\alpha}, \quad (25)$$

where  $\alpha$  is a constant. Czajkowski, McGillis and Krause<sup>36</sup> have shown that such a relation describes the resonant energy transfer cross sections in Rb - Cs collisions with  $\alpha = 2.1 \pm 0.1$ . The  $Q_{21}$  mixing cross sections for collisions between cesium and  $H_2$ ,  $D_2$  and HD molecules, could also be described by Eq. (25) if a resonant transfer of energy into molecular rotation does take place. We shall examine these systems more closely to see if this is the case.

A molecule which is involved in a mixing collision may initially occupy any one of a number of rotational levels and consequently the measured collision numbers  $Z$  represent the sum of the collision numbers for molecules in the various rotational states  $J$ :  $Z = \sum_J Z_J$ . Therefore the total collision number  $Z_{21}$  for the  ${}^2P_{1/2} \leftarrow {}^2P_{3/2}$  mixing

process can be written as:

$$Z_{21} = N V_r Q_{21} \propto V_r \sum_J N_J \sigma_J, \quad (26)$$

where  $\sigma_J$  is the  ${}^2P_{1/2} \leftarrow {}^2P_{3/2}$  mixing cross section appropriate to a molecule in the  $J$ th rotational state at the time of the collision and  $N_J$  is the number of molecules in the  $J$ th state. The sum over  $J$  should include all the rotational levels that have an appreciable population at the temperature of the fluorescence tube ( $314^\circ\text{K}$ ). The measured total cross section  $Q_{21}$  can be then expressed as:

$$Q_{21} \propto \sum_J (N_J/N) \sigma_J, \quad (27)$$

or, using Eq. (25):

$$Q_{21} = k \sum_J (N_J/N) (\delta E)_J^{-\alpha}, \quad (28)$$

where  $k$  is a proportionality constant and  $(\delta E)_J$  refers to the difference between the cesium  ${}^2P$  energy defect and the energy required for the molecule to make a transition from the rotational state  $J$  to a state of higher energy  $J'$ . It is assumed that intercombinations between symmetric and antisymmetric states are strictly forbidden. This selection rule allows only  $\Delta J = 2$  transitions in  $\text{H}_2$  and  $\text{D}_2$ . In the case of  $\text{HD}$ , transitions with  $\Delta J = 1, 2$  are allowed. When  $(\delta E)_J$  is greater than zero, the Boltzmann factor  $\exp[-(\delta E)_J/kT]$  should be included in Eq. (28) since this amount of energy must then be supplied by the translational kinetic energy of the collision partners.

The number of molecules  $N_J$  in the rotational level  $J$  of the lowest vibrational state at the temperature  $T(^{\circ}\text{K})$  is given by:

$$N_J = (N/Q_R) (2t + 1) (2J + 1) \exp[-F(J)/kT]. \quad (29)$$

$F(J)$  is the energy (in  $\text{cm}^{-1}$ ) of the  $J$ th rotational level referred to the  $J = 0$  level and  $t$ , the quantum number of the total nuclear spin of a homonuclear molecule, is given by:

$$t = 2I, 2I - 1, \dots, 0, \quad (30)$$

where  $I$  is the nuclear spin of the nuclei in the molecule. For the heteronuclear molecule HD the expression  $(2t + 1)$  must be replaced by the factor  $(2I_1 + 1)(2I_2 + 1)$  where  $I_1$  and  $I_2$  are the nuclear spins of the two nuclei. The rotational partition function  $Q_R$  is given by the sum:

$$Q_R = \sum_J (2t + 1) (2J + 1) \exp [-F(J)/kT] . \quad (31)$$

The ratio of the number of molecules in the  $J$ th rotational level to the total number of molecules ( $N_J/N$ ), which appears in Eq. (28) can be calculated from Eqs. (29) - (31) using the spectroscopic data given by Herzberg<sup>37</sup> for the molecules  $\text{H}_2$ ,  $\text{D}_2$  and HD.

In order to calculate the  $\delta E$  dependence of the partial cross sections  $\sigma_J$  from Eq. (28) the proportionality constant  $k$  must be known. In view of the equality of the K -  $\text{H}_2$ , K -  $\text{D}_2$  and K - HD mixing cross sections, where no resonant transfer of energy is evident, it has been concluded that the value of  $k$  must be the same for all three molecules. Using in Eq. (28) the experimental values of  $Q_{21}$  for the Cs -  $\text{H}_2$ , Cs -  $\text{D}_2$  and Cs - HD collisions and imposing the condition that  $k$  be the same in all three systems, the values of  $k$  and  $\alpha$  were found to be:  $k = 1.47 \times 10^{-13}$ , and  $\alpha = 0.85 \pm 0.10$  so that the partial cross section for  ${}^2P_{1/2} \leftarrow {}^2P_{3/2}$  mixing can be empirically represented by the equation:

$$\sigma_J = 1.47 (\delta E)_J^{-0.85} \times 10^{-13} \text{ cm}^2 . \quad (32)$$

The degree to which this expression approximates the experimental results can be judged from Table VII where a comparison is made between the experimental total cross sections  $Q_{21}$  and those calculated on the basis of Eqs. (28) and (32). Even though the experimental cross sections were used to find the parameters  $k$  and  $\alpha$ , the close fit which is obtained indicates that Eq. (28) does describe the Cs - H<sub>2</sub>, Cs - D<sub>2</sub> and Cs - HD mixing collisions. Included in Table VII are the calculated cross sections for  $^2P_{1/2} \leftarrow ^2P_{3/2}$  mixing in cesium induced by ortho and para hydrogen collisions at 314°K. These cross sections have not yet been measured but their determination should clarify the role that the molecular rotational levels play in the  $^2P$  mixing process. It does, however, appear that the availability of rotational levels in the range of the  $^2P$  energy defect greatly increases the  $^2P$  mixing probability

TABLE VII

Collision Partners	$Q_{21} (\text{\AA})^2$ Calculated	$Q_{21} (\text{\AA})^2$ Experimental
Cs - H <sub>2</sub>	44	43.8
Cs - D <sub>2</sub>	27	27.8
Cs - HD	33	32.1
Cs-p-H <sub>2</sub> (J = 0 — J = 2)	16	--
Cs-o-H <sub>2</sub> (J = 1 — J = 3)	65	--

and that rotational transitions do occur.

Regardless of the mixing mechanism it is expected from the principle of detailed balancing that the ratio of  $Q_{12}/Q_{21}$  should be given by:

$$Q_{12}/Q_{21} = (g_2/g_1) \exp [-\Delta E/kT] , \quad (33)$$

where  $g_1$  and  $g_2$  are the statistical weights of the  $^2P_{1/2}$  and  $^2P_{3/2}$  states ( $g_1 = 2$ ;  $g_2 = 4$ ) and  $\Delta E$  is the energy defect between them. The expected ratios of  $Q_{12}/Q_{21}$  for potassium and cesium are therefore 1.59 and 0.159, respectively. It can be seen from Tables II and IV that the experimental ratios of  $Q_{12}/Q_{21}$  are in good agreement with those predicted by Eq. (33).

The Cs - N<sub>2</sub>  $^2P$  mixing cross sections are about two orders of magnitude larger than would be expected from Eq. (32). The reason for this may be connected with the assumption, made in the preceding treatment of the Cs - H<sub>2</sub>, D<sub>2</sub> and HD cross sections, that there is little tendency towards a crossing of the potential energy curves of the intermediate complex that correlate with the cesium  $^2P_{1/2}$  and  $^2P_{3/2}$  states. Dickens, Linnett and Sovers<sup>13</sup> have shown that only under these circumstances can a correlation be expected between the efficiency of energy transfer and the coincidence of a molecular energy level with the energy difference between the initial and final electronic states. It would seem that in the Cs - N<sub>2</sub> system there is a near crossing of the  $^2P_J$  potential energy curves: the Cs - N<sub>2</sub> system is the only system in which the quenching reaction, which is presumed to proceed by way of potential curve crossings, is more efficient than the mixing reaction. In this

case then, mixing between the  $^2P$  states may well be accomplished by a mechanism similar to that of the quenching reaction.

APPENDIX A  
EXPERIMENTAL DATA

K - HD DATA

P (Torr)	$\eta_1$	$\eta_2$	$(I_o/I)_1$	$(I_o/I)_2$
.025	.0144	.0225	1.0620	1.0240
.041	.0219	.0350	1.0500	1.0380
.096	.0534	.0805	1.1020	1.0700
.117	.0593	.0950	1.1500	1.1080
.120	.0644	.0965	1.1600	1.0970
.140	.0722	.1220	1.1980	1.1090
.160	.0828	.1290	1.1810	1.1200
.182	.0945	.1460	1.2200	1.1250
.183	.0887	.1470	1.2220	1.1400
.186	.0884	.1500	1.2250	1.1330
.210	.1057	.1650	1.2630	1.1660
.280	.1303	.2100	1.3250	1.2000
.312	.1460	.2350	1.3500	1.2370
.315	.1460	.2350	1.3600	1.2400
.320	.1430	.2350	1.3600	1.2030
.355	.1570	.2560	1.3920	1.2700
.366	.1610	.2610	1.4100	1.2700
.395	.1767	.2810	1.4380	1.2880
.421	.1703	.2900	1.4600	1.2630
.447	.1875	.3010	1.4850	1.3120
.463	.1800	.3130	1.5000	1.3020
.477	.1930	.3160	1.5100	1.3400
.495	.1960	.3260	1.5820	1.3500
.525	.2075	.3475	1.5800	1.3660
.535	.2060	.3600	1.6300	1.3800
.603	.2245	.3890	1.6720	1.4800
.636	.2385	.3990	1.7350	1.5120
.660	.2335	.4010	1.7600	1.5070
.705	.2330	.4225	1.8000	1.4700
.760	.2445	.4310	1.9040	1.5440
.822	.2720	.4440	1.9600	1.6400
.835	.2670	.4440	1.9600	1.6440
.950	.2685	.4990	2.1600	1.7400
.955	.2855	.4990	2.1600	1.7800
.970	.2855	.5050	2.1700	1.7300
1.030	.2942	.5200	2.2800	1.8800
1.050	.2940	.5140	2.3350	1.8700
1.060	.2970	.5140	2.3350	1.9000
1.110	.2990	.5340	2.3800	1.9450
1.120	.2935	.5340	2.3800	1.9220
1.200	.3165	.5740	2.6800	2.0050

K - H<sub>2</sub> DATA

P (Torr)	$\eta_1$	$\eta_2$	$(I_o/I)_1$	$(I_o/I)_2$
.025	.0184	.0265	1.0300	1.0490
.047	.0343	.0500	1.0850	1.0530
.070	.0493	.0725	1.0975	1.0835
.072	.0499	.0730	1.0980	1.0850
.091	.0614	.0895	1.1360	1.1010
.112	.0779	.1110	1.1600	1.0990
.115	.0789	.1175	1.1630	1.1250
.125	.0861	.1227	1.1660	1.1160
.125	.0820	.1275	1.1700	1.1430
.142	.0960	.1419	1.1840	1.1290
.163	.1100	.1630	1.2110	1.1690
.168	.1104	.1634	1.2130	1.1620
.195	.1181	.1775	1.2400	1.1830
.214	.1263	.1990	1.2630	1.1650
.230	.1438	.2100	1.2800	1.2010
.248	.1429	.2240	1.3000	1.2210
.250	.1500	.2260	1.3050	1.2220
.260	.1550	.2310	1.3220	1.2320
.290	.1680	.2600	1.3390	1.2410
.292	.1612	.2550	1.3500	1.2335
.308	.1725	.2680	1.3570	1.2400
.320	.1800	.2775	1.3880	1.2530
.334	.1800	.2850	1.4000	1.2750
.360	.2000	.3020	1.4200	1.2970
.362	.1948	.3020	1.4200	1.2900
.394	.2015	.3270	1.4550	1.3090
.418	.2145	.3420	1.4830	1.3360
.428	.2155	.3490	1.4950	1.3430
.480	.2405	.3720	1.5750	1.3760
.497	.2407	.3885	1.5600	1.4080
.520	.2450	.4020	1.6000	1.4120
.580	.2680	.4350	1.7000	1.4850
.625	.2825	.4575	1.7500	1.5320
.634	.2675	.4610	1.7750	1.5250
.720	.2885	.4950	1.8600	1.5950
.776	.3122	.5150	1.9300	1.6660
.802	.3000	.5250	1.9500	1.6900
.857	.3190	.5475	2.0200	1.7600
.960	.3210	.5775	2.1700	1.8420
1.030	.3590	.6000	2.2420	1.9560
1.190	.3800	.6400	2.5750	2.1300
1.200	.3800	.6550	2.5500	2.1600

K - D<sub>2</sub> DATA

P (Torr)	$\eta_1$	$\eta_2$	$(I_o/I)_1$	$(I_o/I)_2$
.022	.0111	.0150	1.0150	1.0000
.025	.0131	.0160	1.0200	1.0110
.029	.0143	.0217	1.0150	1.0000
.040	.0197	.0295	1.0270	1.0200
.045	.0230	.0310	1.0300	1.0280
.066	.0330	.0506	1.0245	1.0420
.077	.0366	.0517	1.0570	1.0490
.082	.0413	.0550	1.0600	1.0460
.085	.0398	.0652	1.0680	1.0410
.100	.0469	.0704	1.0790	1.0470
.108	.0499	.0753	1.0725	1.0610
.108	.0499	.0775	1.0725	1.0500
.110	.0519	.0810	1.0800	1.0670
.133	.0644	.0940	1.1000	1.0650
.139	.0665	.0950	1.1050	1.0820
.145	.0707	.1007	1.1060	1.0670
.145	.0685	.1000	1.1050	1.0880
.155	.0725	.1041	1.1310	1.0710
.160	.0762	.1110	1.1200	1.0880
.165	.0755	.1147	1.1200	1.0880
.181	.0849	.1316	1.1370	1.1050
.188	.0858	.1301	1.1450	1.0970
.190	.0866	.1301	1.1450	1.0960
.202	.0946	.1342	1.1540	1.1120
.218	.0999	.1470	1.1600	1.1200
.221	.1030	.1489	1.1720	1.1190
.230	.1040	.1550	1.1700	1.1290
.239	.1097	.1668	1.1820	1.1330
.240	.1061	.1540	1.1820	1.0990
.259	.1116	.1740	1.1950	1.1190
.262	.1114	.1729	1.1212	1.1380
.289	.1284	.1900	1.2140	1.1550
.291	.1242	.1990	1.2140	1.1240
.292	.1251	.1930	1.2140	1.1600
.340	.1364	.2200	1.2550	1.1800
.350	.1456	.2346	1.2640	1.1870
.360	.1541	.2310	1.2750	1.1730
.375	.1502	.2390	1.3270	1.2010
.410	.1688	.2630	1.3010	1.2220
.428	.1762	.2650	1.3200	1.2190
.445	.1708	.2750	1.3500	1.2390
.500	.1978	.3050	1.3700	1.2500
.511	.2019	.3100	1.3800	1.2460
.525	.1932	.3175	1.3900	1.2760
.615	.2247	.3600	1.4600	1.2980
.621	.2250	.3650	1.4700	1.3150
.660	.2335	.3750	1.5000	1.3220

K - D<sub>2</sub> DATA (continued)

P (Torr)	$\eta_1$	$\eta_2$	$(I_o/I)_1$	$(I_o/I)_2$
.765	.2538	.4150	1.5900	1.3430
.765	.2538	.4250	1.5900	1.3690
.785	.2570	.4275	1.6000	1.3970
.810	.2740	.4410	1.6210	1.4150
.863	.2700	.4610	1.6860	1.3900
1.010	.2805	.5040	1.8010	1.4170

K - N<sub>2</sub> DATA

P (Torr)	$\eta_1$	$\eta_2$	$(I_o/I)_1$	$(I_o/I)_2$
.042	.0142	.0200	1.0400	1.0250
.046	.0143	.0229	1.0300	1.0200
.064	.0200	.0310	1.0430	1.0370
.065	.0204	.0310	1.0530	1.0340
.108	.0326	.0524	1.0770	1.0600
.127	.0393	.0596	1.1100	1.0700
.151	.0463	.0706	1.1070	1.0910
.162	.0490	.0750	1.1120	1.0810
.165	.0491	.0758	1.1060	1.1000
.199	.0610	.0920	1.1375	1.1150
.200	.0566	.0931	1.1400	1.1000
.214	.0644	.0936	1.1550	1.1260
.235	.0706	.1030	1.1570	1.1310
.236	.0694	.1053	1.1570	1.1350
.258	.0750	.1139	1.1830	1.1310
.260	.0738	.1139	1.1830	1.1430
.271	.0770	.1171	1.1980	1.1490
.300	.0826	.1280	1.2030	1.1540
.310	.0869	.1292	1.2010	1.1550
.313	.0883	.1320	1.2110	1.1510
.328	.0881	.1400	1.2230	1.1640
.330	.0899	.1400	1.2230	1.1670
.340	.0935	.1428	1.2260	1.1850
.340	.0938	.1428	1.2260	1.1540
.368	.0951	.1530	1.2480	1.1700
.377	.1036	.1553	1.2520	1.1880
.410	.1084	.1675	1.2750	1.2080
.411	.1086	.1675	1.2750	1.2300
.447	.1168	.1820	1.2950	1.2100
.459	.1141	.1850	1.3000	1.2210
.470	.1209	.1875	1.3050	1.2420
.480	.1211	.1895	1.3090	1.2350
.560	.1330	.2130	1.3630	1.2600
.569	.1398	.2170	1.3700	1.2640
.615	.1517	.2300	1.3950	1.2910
.702	.1578	.2520	1.4420	1.3200
.710	.1620	.2550	1.4490	1.3260
.720	.1606	.2570	1.4600	1.3440
.800	.1676	.2770	1.5050	1.3860
.800	.1758	.2770	1.5050	1.3640
.940	.1916	.3100	1.5600	1.4200
1.000	.1995	.3220	1.6000	1.4350
1.060	.2025	.3230	1.6300	1.4730
1.112	.2100	.3480	1.6990	1.4900
1.300	.2154	.3750	1.7800	1.5425
1.340	.2310	.3800	1.8100	1.5620
1.850	.2565	.4500	2.0400	1.6960

## Cs - HD DATA

P (Torr)	$\eta_1$	$\eta_2$
0.008	0.00468	0.00093
0.021	0.01179	0.00225
0.027	0.01698	0.00284
0.047	0.02785	0.00455
0.055	0.02980	0.00474
0.057	0.03180	0.00526
0.058	0.03520	0.00579
0.067	0.03660	0.00599
0.076	0.03970	0.00705
0.085	0.04810	0.00766
0.110	0.05200	0.00856
0.111	0.05280	0.00878
0.123	0.05800	0.00953
0.128	0.06325	0.00980
0.143	0.07040	0.01180
0.164	0.08370	0.01299
0.194	0.08930	0.01479
0.217	0.10770	0.01718
0.221	0.10800	0.01780
0.238	0.11800	0.01945
0.279	0.13400	0.02108
0.289	0.13810	0.02195
0.309	0.14700	0.02290
0.331	0.15300	0.02510
0.340	0.16220	0.02478
0.380	0.18100	0.02810
0.390	0.18380	0.02760
0.429	0.20000	0.03120
0.439	0.20580	0.03170
0.469	0.21220	0.03325
0.510	0.23750	0.03560
0.535	0.24750	0.03490
0.545	0.25400	0.03790
0.604	0.26900	0.03900
0.630	0.27800	0.04070
0.646	0.28900	0.04040
0.700	0.32600	0.04560
0.715	0.32650	0.04490
0.734	0.32800	0.04590
0.780	0.34600	0.04610
0.840	0.37200	0.05030
0.887	0.37800	0.05060
0.935	0.39400	0.05130
0.958	0.40700	0.05250
0.960	0.40700	0.05225
1.010	0.43300	0.05680
1.010	0.42700	0.05510

Cs - H<sub>2</sub> DATA

P (Torr)	$\eta_1$	$\eta_2$
0.021	0.01345	0.00276
0.022	0.01075	0.00204
0.028	0.02010	0.00406
0.044	0.03835	0.00712
0.045	0.03900	0.00714
0.048	0.03570	0.00612
0.064	0.05510	0.00947
0.071	0.05740	0.01030
0.072	0.06040	0.01047
0.160	0.08990	0.01310
0.106	0.08170	0.01399
0.115	0.09170	0.01452
0.119	0.09580	0.01524
0.129	0.10120	0.01610
0.140	0.10540	0.01620
0.151	0.11770	0.01812
0.160	0.12650	0.01918
0.169	0.14440	0.02195
0.175	0.14710	0.02290
0.181	0.14480	0.02295
0.194	0.15200	0.02340
0.201	0.15920	0.02422
0.221	0.16700	0.02485
0.229	0.18310	0.02765
0.236	0.18450	0.02830
0.256	0.19520	0.03137
0.265	0.19720	0.03090
0.270	0.22800	0.03300
0.277	0.20900	0.03210
0.290	0.22850	0.03530
0.312	0.23730	0.03580
0.321	0.23050	0.03480
0.345	0.26220	0.03890
0.368	0.29200	0.04210
0.401	0.28750	0.04420
0.423	0.31450	0.04480
0.425	0.32800	0.04540
0.450	0.31225	0.04320
0.478	0.34450	0.04680
0.506	0.35650	0.04850
0.521	0.39500	0.05025
0.523	0.35950	0.04910
0.580	0.39800	0.05340
0.598	0.41600	0.05500
0.601	0.40300	0.05500
0.610	0.43400	0.05710
0.641	0.44400	0.05790

Cs - H<sub>2</sub> DATA (continued)

P (Torr)	$\eta_1$	$\eta_2$
0.658	0.45100	0.05890
0.662	0.45800	0.05890
0.664	0.45500	0.05840
0.795	0.51900	0.06640
0.803	0.52300	0.06570
0.820	0.52300	0.06640
0.930	0.57400	0.07030
0.935	0.57100	0.07080
1.010	0.60100	0.07240
1.080	0.61500	0.07540
1.085	0.62100	0.07590

P (Torr)	$\eta_1$	$\eta_2$
0.007	0.00046	0.00013
0.010	0.00191	0.00042
0.020	0.00463	0.00094
0.022	0.00588	0.00123
0.030	0.00862	0.00197
0.044	0.01350	0.00255
0.058	0.02235	0.00367
0.067	0.02290	0.00406
0.082	0.03180	0.00553
0.100	0.03260	0.00555
0.106	0.03680	0.00616
0.118	0.04160	0.00716
0.120	0.04430	0.00740
0.120	0.04210	0.00714
0.125	0.04450	0.00748
0.140	0.05370	0.00869
0.157	0.05870	0.00943
0.165	0.06080	0.01000
0.168	0.06480	0.01036
0.190	0.06990	0.01135
0.226	0.08160	0.01297
0.231	0.08730	0.01390
0.267	0.09690	0.01545
0.280	0.10280	0.01590
0.280	0.10120	0.01555
0.300	0.10570	0.01645
0.301	0.10890	0.01698
0.335	0.12050	0.01980
0.365	0.12400	0.02000
0.375	0.13250	0.02075
0.400	0.14520	0.02341
0.405	0.14030	0.02180
0.410	0.14200	0.02200
0.467	0.16345	0.02565
0.510	0.17300	0.02565
0.545	0.18050	0.02770
0.555	0.19520	0.02865
0.560	0.19750	0.02955
0.580	0.19200	0.02855
0.672	0.21600	0.03170
0.680	0.22900	0.03470
0.727	0.23850	0.03600
0.775	0.23850	0.03570
0.800	0.26200	0.03830
0.873	0.26400	0.03880
0.905	0.27200	0.04220
0.965	0.30100	0.04425
1.160	0.34400	0.04910

Cs - N<sub>2</sub> DATA

P (Torr)	$\eta_1$	$\eta_2$
0.021	0.00247	0.00062
0.021	0.00282	0.00057
0.028	0.00372	0.00099
0.034	0.00468	0.00100
0.047	0.00678	0.00151
0.047	0.00676	0.00162
0.050	0.00675	0.00143
0.063	0.00918	0.00186
0.064	0.00907	0.00208
0.066	0.00876	0.00186
0.069	0.00845	0.00192
0.070	0.01010	0.00215
0.075	0.01010	0.00206
0.104	0.01311	0.00286
0.110	0.01472	0.00297
0.116	0.01510	0.00306
0.139	0.01760	0.00355
0.156	0.01740	0.00354
0.164	0.01880	0.00373
0.169	0.01911	0.00379
0.180	0.02185	0.00403
0.220	0.02483	0.00486
0.238	0.02722	0.00535
0.265	0.03048	0.00572
0.268	0.02957	0.00557
0.289	0.03290	0.00617
0.293	0.03258	0.00628
0.352	0.04030	0.00717
0.377	0.03870	0.00781
0.382	0.04110	0.00783
0.395	0.04390	0.00821
0.400	0.04400	0.00831
0.415	0.04560	0.00851
0.432	0.04610	0.00875
0.458	0.04930	0.00900
0.506	0.05460	0.00949
0.518	0.05590	0.01000
0.580	0.06130	0.01052
0.594	0.05940	0.01040
0.668	0.06650	0.01167
0.674	0.06790	0.01230
0.705	0.07300	0.01170
0.755	0.07440	0.01288
0.773	0.07400	0.01297
0.779	0.07290	0.01272
0.835	0.07900	0.01360

Cs - N<sub>2</sub> DATA (continued)

P (Torr)	$\eta_1$	$\eta_2$
0.862	0.08040	0.01360
0.938	0.08490	0.01459
0.943	0.08610	0.01459
1.010	0.08910	0.01538
1.110	0.09575	0.01615
1.110	0.09700	0.01629

## APPENDIX B

### ITERATIVE METHOD OF CALCULATING THE COLLISION NUMBERS $Z_{ab}$

First approximations to the collision numbers were obtained using Eqs. (19) and (20) and the first three terms on the right hand side of Eqs. (14) and (15) to solve for  $Z_{10}$  and  $Z_{20}$ :

$$Z_{10} = \frac{(1 + C) (R_1 - 1 - \tau_1 D) - (\tau_1 / \tau_2) (R_2 - 1 - \tau_2 A) E}{\tau_1 [(1 + C)^2 - BE]}, \quad (B1)$$

$$Z_{20} = \frac{(1 + C) (R_2 - 1 - \tau_2 A) - (\tau_2 / \tau_1) (R_1 - 1 - \tau_1 D) B}{\tau_2 [(1 + C)^2 - BE]}, \quad (B2)$$

where  $(I_0/I)_1$  has been replaced by  $R_1$ .  $Z_{12}$  and  $Z_{21}$  were then calculated by substituting Eqs. (B1) and (B2) into Eqs. (19) and (20). These initial values of  $Z_{ab}$  were then used to compute the fourth terms in Eqs. (14) and (15) which were then added to  $R_1$  and  $R_2$  respectively. Using the new values of  $R_1$  and  $R_2$ , in conjunction with Eqs. (B1), (B2), (19) and (20), second approximations to  $Z_{ab}$  were obtained. This procedure was continued until successive approximations differed by less than 0.1 per cent. Convergence was rapid, usually requiring less than five iterations.

## APPENDIX C

### CALCULATION OF THE QUENCHING CROSS SECTIONS

#### $Q_{10}$ AND $Q_{20}$ FROM $\eta$ -VALUES

The collision numbers  $Z_{12}$  and  $Z_{21}$  obtained from the first term in Eqs. (19) and (20) were generally non-linear at high gas pressures. The departure from the expected linear behaviour (the broken line) was attributed to the neglected quenching terms and therefore the difference between the curves,  $\Delta$ , was defined as:

$$\Delta_{21} = Z_{21} - A = BZ_{10} + CZ_{20}, \quad (C1)$$

$$\Delta_{12} = Z_{12} - D = EZ_{20} + CZ_{10}. \quad (C2)$$

The collision numbers  $Z_{10}$  and  $Z_{20}$  are then:

$$Z_{10} = (\tau_2/\tau_1) (\Delta_{21}/\eta_1) - \Delta_{12}, \quad (C3)$$

$$Z_{20} = (\tau_1/\tau_2) (\Delta_{12}/\eta_2) - \Delta_{21}. \quad (C4)$$

The quenching cross sections  $Q_{10}$  and  $Q_{20}$  were calculated point-for-point from Eqs. (C3), (C4) and (22).

## BIBLIOGRAPHY

1. L. Krause, Appl. Opt. 5, 1375 (1966).
2. R. W. Wood and F. L. Mohler, Phys. Rev. 11, 70 (1918).
3. W. Lochte-Holtgreven, Z. Physik 47, 363 (1928).
4. A. C. G. Mitchell and M. W. Zemansky, Resonance Radiation and Excited Atoms (Cambridge University Press, New York, 1961).
5. P. Pringsheim, Fluorescence and Phosphorescence (Interscience Publishers, Inc., New York, 1949).
6. K. J. Laidler, The Chemical Kinetics of Excited States (Oxford University Press, New York, 1955).
7. H. P. Hooymayers and C. Alkemade, J.Q.S.R.T. 6, 501 (1966).
8. J. Gatzke, Z. Physik. Chem. 223, 321 (1963).
9. W. M. Smith, J. A. Stewart and G. W. Taylor, Can. J. Chem. 32, 961 (1954).
10. J. Pitre, F.S.C., Ph.D. Thesis, University of Windsor, 1967 (unpublished).
11. H. Kallmann and F. London, Z. Physik. Chem. B2, 207 (1929).
12. P. M. Morse and E. C. G. Stueckelberg, Ann. Phys. Lpz. 9, 579 (1931).
13. P. G. Dickens, J. W. Linnett and O. Sovers, Discussions Faraday Soc. 33, 52 (1962).
14. G. Karl, P. Kruus and J. C. Polanyi, J. Chem. Phys. 46, 224 (1967).
15. O. K. Rice, Phys. Rev. 37, 1187, 1551 (1931).
16. J. L. Magee and T. Ri, J. Chem. Phys. 9, 638 (1941).
17. K. J. Laidler, J. Chem. Phys. 10, 43 (1942).
18. M. D. Scheer and J. Fine, J. Chem. Phys. 36, 1264 (1962).
19. A. B. Callear, Appl. Opt. (Chem. Laser Suppl.) 1965, 145.

20. G. D. Chapman and L. Krause, *Can. J. Phys.* 44, 753 (1966).
21. M. Czajkowski and L. Krause, *Can. J. Phys.* 43, 1259 (1965).
22. O. Stern and M. Volmer, *Physik. Z.* 20, 183 (1919).
23. R. Seiwert, *Ann. Physik* 18, 54 (1956).
24. R. J. Atkinson, G. D. Chapman and L. Krause, *J. Opt. Soc. Am.* 55, 1269 (1965).
25. D. H. Burling, M. Czajkowski and L. Krause, *J. Opt. Soc. Am.* (in print).
26. J. B. Taylor and I. Langmuir, *Phys. Rev.* 51, 753 (1937).
27. K. Nakayama and H. Ishii, *Transactions of the Eighth National Vacuum Symposium* (Pergamon Press, Inc., New York, 1962), Vol. I, p. 519.
28. E. Rothe, *J. Vacuum Sci. Tech.* 1, 66 (1964).
29. J. K. Link, *J. Opt. Soc. Am.* 56, 1195 (1966).
30. Landolt-Bornstein, *Zahlwerte und Funktionen* (Springer-Verlag, Berlin, 1950).
31. S. Ch'en and M. Takeo, *Rev. Mod. Phys.* 29, 20 (1957).
32. P. P. Feofilov, *The Physical Basis of Polarized Emission* (Consultants Bureau, New York, 1961).
33. B. P. Kibble, G. Copley and L. Krause, *Phys. Rev.* 159-1, 11 (1967).
34. J. Callaway and E. Bauer, *Phys. Rev.* 140, 1072 (1965).
35. J. Franck, *Naturwiss.* 14, 211 (1929).
36. M. Czajkowski, D. A. McGillis and L. Krause, *Can. J. Phys.* 44, 741 (1966).
37. G. Herzberg, *Spectra of Diatomic Molecules* (D. van Nostrand Company, Inc., New York, 1957).

#### VITA AUCTORIS

The author was born on May 4, 1941, in Detroit, Michigan. After graduation from Detroit Catholic Central High School in 1959, he enrolled at Assumption University and in 1963 received a B.Sc. degree. He then entered the Faculty of Graduate Studies at the University of Windsor as a Province of Ontario Graduate Fellow and received his M.Sc. degree in Physics in 1965. In 1964 he married his wife, Suzanne, and in 1965 was presented with a daughter, Erin Lynn.